PHYSICAL REVIEW D **94,** 085022 (2016)

Maxwell-Jüttner distribution for rigidly rotating flows in spherically symmetric spacetimes using the tetrad formalism

Victor E. Ambruş[*] and Ion I. Cotăescu[†]

Department of Physics, West University of Timişoara, Bd. Vasile Pârvan 4, Timisoara 300223, Romania

(Received 3 June 2016; published 21 October 2016)

We consider rigidly rotating states in thermal equilibrium on static spherically symmetric spacetimes. Using the Maxwell-Jüttner equilibrium distribution function, constructed as a solution of the relativistic Boltzmann equation, the equilibrium particle flow four-vector, stress-energy tensor and the transport coefficients in the Marle model are computed. Their properties are discussed in view of the topology of the speed-of-light surface induced by the rotation for two classes of spacetimes: maximally symmetric (Minkowski, de Sitter and anti-de Sitter) and nonrotating black hole (Schwarzschild and Reissner-Nordström) spacetimes. To facilitate our analysis, we employ a nonholonomic comoving tetrad field, obtained unambiguously by applying a Lorentz boost on a fixed background tetrad.

DOI: 10.1103/PhysRevD.94.085022

I. INTRODUCTION

Because of their simplicity, rigidly rotating systems in thermal equilibrium represent attractive toy models which can be used to gain insight on the physical features of more complex systems or geometries which exhibit rotation (e.g. rotating Kerr black holes). Such systems can be interesting also from a quantum field theory point of view, where the definition of vacuum states or states at finite temperature is still an open field (for some recent results, see Ref. [1] and references therein).

On Minkowski spacetime, such systems were studied using both kinetic theory and quantum field theory [2–19] and the quantum corrections can be obtained analytically [14,15,17]. In this paper, we use the relativistic Boltzmann equation to study the equilibrium states and the transport coefficients of fluids undergoing rigid rotation on static spherically symmetric background spacetimes, as well as to discuss the topology of the speed of light surface (SOL) which forms due to the rotation.

In order to obtain expressions for the transport coefficients, the Marle model is employed for the Boltzmann collision integral [20]. To facilitate our analysis, we employ nonholonomic tetrad fields [21–23] with respect to which the mass shell condition for the momentum four-vector becomes independent of the background metric, while the calculation of the transport coefficients becomes identical with that on the Minkowski spacetime [6]. The tetrad of the comoving frame is obtained by applying a pure Lorentz boost (i.e. without rotation) on the tetrad of the background metric [24]. The only degrees of freedom available in this procedure correspond to choosing the gauge for the fixed tetrad. Our formulation is sufficiently general to encompass previously studied examples, such as the Minkowski [17] and Schwarzschild [25,26] spacetimes. We specialize our results to the cases of maximally symmetric spacetimes (Minkowski, de Sitter and anti-de Sitter spaces), as well as for nonrotating black hole spacetimes (i.e. the Schwarzschild and Reissner-Nordström spacetimes).

In Sec. II, we discuss the tetrad formalism, which we apply to obtain the transport coefficients in the Marle model. The construction of the comoving frame for rigidly rotating flows on spherically symmetric spaces is presented in Sec. III, while Sec. IV is dedicated to the discussion of rigidly rotating thermal states on maximally symmetric and Schwarzschild and Reissner-Nordström black hole spacetimes by considering the properties of the Killing horizons seen by rotating observers. Section V concludes this paper.

II. THE RELATIVISTIC BOLTZMANN EQUATION

We start this section by presenting in Sec. II A a technique for defining the comoving frame with no unspecified degrees of freedom, which relies on a fixed tetrad field corresponding to the (arbitrary) background spacetime.

Section II B reviews the Boltzmann equation written with respect to tetrad fields in conservative form, as described in Ref. [23]. Details regarding the transition from the generally covariant Boltzmann equation to the Boltzmann equation with respect to tetrad fields, as well as from this latter form to the conservative form of the Boltzmann equation, are presented in Appendices A and B, respectively.

Section II C introduces the Maxwell-Jüttner distribution for local thermodynamic equilibrium, as well as the conditions that the chemical potential, temperature and four-velocity must satisfy in order for the fluid to be in global thermodynamic equilibrium.

[*]victor.ambrus@e-uvt.ro
[†]icotaescu@yahoo.com

Section II D ends this section by introducing the transport coefficients arising when the Marle model is used for the collision integral, which are calculated starting from the Boltzmann equation in conservative form in a manner analogous to that employed on flat space [6]. The expressions for the resulting coefficients, defined by using a covariant generalization [27] of their flat spacetime definitions, are identical to those obtained in flat spacetime.

A. Comoving frame

For a fixed spacetime having the line element

$$ds^2 = g_{\mu\nu}dx^\mu dx^\nu, \tag{2.1}$$

an orthonormal frame $\{e_{\tilde{a}}\}$ can be chosen such that the metric is locally flat:

$$g_{\mu\nu}e^\mu_{\tilde{a}}e^\nu_{\tilde{b}} = \eta_{\tilde{a}\,\tilde{b}}, \tag{2.2}$$

where $\eta_{\tilde{a}\,\tilde{b}} = \mathrm{diag}(-1,1,1,1)$ is the metric of the Minkowskian model of this spacetime. The tetrad frame vectors $e^\mu_{\tilde{a}}$ uniquely determine a set of covectors (one-forms) $\{\omega^{\tilde{a}}\}$ through [24]:

$$\langle e_{\tilde{b}}, \omega^{\tilde{a}}\rangle \equiv \omega^{\tilde{a}}_\mu e^\mu_{\tilde{b}} = \delta^{\tilde{a}}{}_{\tilde{b}}. \tag{2.3}$$

There are 6 degrees of freedom in choosing the tetrad, due to the invariance of Eq. (2.2) under Lorentz transformations. However, we consider that the tetrad $\{e_{\tilde{a}}\}$ is fixed in some predefined gauge, such that it can serve as a reference tetrad for the future development in this chapter.

A comoving frame is defined as an orthonormal frame $\{e_{\hat{\alpha}}\}$ with respect to which the fluid four-velocity is

$$u^{\hat{\alpha}} \equiv u^\mu \omega^{\hat{\alpha}}_\mu = (1,0,0,0), \tag{2.4}$$

where $\{\omega^{\hat{\alpha}}\}$ are the covectors corresponding to the tetrad vectors $\{e_{\hat{\alpha}}\}$. Equation (2.4) implies

$$e^\mu_{\hat{0}} = u^\mu. \tag{2.5}$$

Equation (2.5) reduces the number of degrees of freedom in Eq. (2.2) to 3. We eliminate these degrees of freedom by requiring that the comoving frame $\{e_{\hat{a}}\}$ is obtained from the local frame $\{e_{\tilde{a}}\}$ by applying a pure Lorentz boost $L^{\tilde{a}}{}_{\hat{\alpha}}$, such that

$$e_{\hat{\alpha}} = e_{\tilde{a}}L^{\tilde{a}}{}_{\hat{\alpha}}. \tag{2.6}$$

The components $L^{\tilde{a}}{}_{\hat{0}}$ can be obtained by contracting Eq. (2.5) with $\omega^{\tilde{a}}_\mu$:

$$L^{\tilde{a}}{}_{\hat{0}} = u^{\tilde{a}} \equiv u^\mu \omega^{\tilde{a}}_\mu. \tag{2.7}$$

The above equation fixes all 3 degrees of freedom of the genuine Lorentz boost $L^{\tilde{a}}{}_{\hat{\alpha}}$, which can be written as follows:

$$L^{\tilde{a}}{}_{\hat{\alpha}} = \begin{pmatrix} u^{\tilde{0}} & u_{\tilde{j}} \\ u^{\tilde{i}} & \delta^{\tilde{i}}{}_{\tilde{j}} + \dfrac{u^{\tilde{i}}u_{\tilde{j}}}{u^{\tilde{0}}+1} \end{pmatrix}. \tag{2.8}$$

It can be checked that $L^{\tilde{a}}{}_{\hat{\beta}}$ is indeed a pseudo-orthogonal matrix:

$$\eta_{\tilde{a}\,\tilde{b}}L^{\tilde{a}}{}_{\hat{\alpha}}L^{\tilde{b}}{}_{\hat{\beta}} = \eta_{\hat{\alpha}\hat{\beta}}, \qquad \eta^{\hat{\alpha}\hat{\beta}}L^{\tilde{a}}{}_{\hat{\alpha}}L^{\tilde{b}}{}_{\hat{\beta}} = \eta^{\tilde{a}\,\tilde{b}}, \tag{2.9}$$

satisfying $L^T = L$ [28].

B. Conservative relativistic Boltzmann equation

The relativistic Boltzmann equation with respect to arbitrary coordinate systems on arbitrary geometries can be written as [6,27,29]

$$p^\mu \frac{\partial f}{\partial x^\mu} - \Gamma^i{}_{\mu\nu}p^\mu p^\nu \frac{\partial f}{\partial p^i} = C[f], \tag{2.10}$$

where $f \equiv f(x^\mu, p^i)$ is the Boltzmann distribution function, x^μ represent spacetime coordinates and $p^\mu = (p^0, p^i)$ are the components of the particle four-momentum vector. The time component p^0 of the momentum 4-vector is fixed by the mass-shell condition:

$$g_{\mu\nu}p^\mu p^\nu = -m^2, \tag{2.11}$$

where $g_{\mu\nu}$ are the components of the spacetime metric. The connection coefficients $\Gamma^i{}_{\mu\nu}$ appearing in Eq. (2.10) have the following expression with respect to a coordinate frame:

$$\Gamma^\lambda{}_{\mu\nu} = \frac{1}{2}g^{\lambda\sigma}(g_{\sigma\mu,\nu} + g_{\sigma\nu,\mu} - g_{\mu\nu,\sigma}), \tag{2.12}$$

where a comma denotes differentiation with respect to the coordinates, e.g. $g_{\sigma\mu,\nu} \equiv \partial_\nu g_{\sigma\mu} \equiv \frac{\partial g_{\sigma\mu}}{\partial x^\nu}$.

The Boltzmann equation (2.10) can be expressed with respect to the tetrad components of the momentum vector as follows:

$$p^{\hat{\alpha}}e^\mu_{\hat{\alpha}}\frac{\partial f}{\partial x^\mu} - \Gamma^{\hat{i}}{}_{\hat{\alpha}\hat{\beta}}p^{\hat{\alpha}}p^{\hat{\beta}}\frac{\partial f}{\partial p^{\hat{i}}} = \mathcal{C}[f]. \tag{2.13}$$

For more details on the relation between Eqs. (2.10) and (2.13), we refer the reader to Appendix A. The connection coefficients $\Gamma^{\hat{\gamma}}{}_{\hat{\alpha}\hat{\beta}}$ appearing in Eq. (2.13) can be obtained using

$$\Gamma^{\hat{\gamma}}{}_{\hat{\alpha}\hat{\beta}} = \eta^{\hat{\gamma}\hat{\rho}}(c_{\hat{\rho}\hat{\alpha}\hat{\beta}} + c_{\hat{\rho}\hat{\beta}\hat{\alpha}} - c_{\hat{\alpha}\hat{\beta}\hat{\rho}}), \tag{2.14}$$

where the Cartan coefficients can be calculated from the commutators of the tetrad vectors [24]:

$$c_{\hat{\alpha}\hat{\beta}}{}^{\hat{\gamma}} = \langle [e_{\hat{\alpha}}, e_{\hat{\beta}}], \omega^{\hat{\gamma}} \rangle. \tag{2.15}$$

In order to derive transport equations for macroscopic quantities, we follow Ref. [23] and express Eq. (2.13) in conservative form:

$$\frac{1}{\sqrt{-g}} \partial_\mu (\sqrt{-g} p^{\hat{\alpha}} e^\mu_{\hat{\alpha}} f) - p^{\hat{0}} \frac{\partial}{\partial p^{\hat{i}}} \left(\Gamma^{\hat{i}}{}_{\hat{\alpha}\hat{\beta}} \frac{p^{\hat{\alpha}} p^{\hat{\beta}}}{p^{\hat{0}}} f \right) = C[f]. \tag{2.16}$$

For completeness, we provide the details of the derivation of the transition from Eq. (2.13) to Eq. (2.16) in Appendix B. The form (2.16) of the Boltzmann equation is particularly convenient from a numerical point of view, being directly amenable to finite-element or finite-volume numerical methods. Furthermore, Eq. (2.16) can be used to easily derive transport equations for the moments $T^{\hat{\alpha}_1 \ldots \hat{\alpha}_{n+1}}$ of f:

$$\nabla_{\hat{\alpha}_{n+1}} T^{\hat{\alpha}_1 \hat{\alpha}_2 \ldots \hat{\alpha}_n \hat{\alpha}_{n+1}} = \int \frac{d^3 p}{p^{\hat{0}}} C[f] p^{\hat{\alpha}_1} \ldots p^{\hat{\alpha}_n}, \tag{2.17}$$

where

$$T^{\hat{\alpha}_1 \hat{\alpha}_2 \ldots \hat{\alpha}_n \hat{\alpha}_{n+1}} \equiv \int \frac{d^3 p}{p^{\hat{0}}} f p^{\hat{\alpha}_1} \ldots p^{\hat{\alpha}_n} p^{\hat{\alpha}_{n+1}}. \tag{2.18}$$

In particular, the conservation equation for the particle four-flow $N^\alpha \equiv T^{\hat{\alpha}}$ and stress-energy tensor $T^{\hat{\alpha}\hat{\beta}}$ can be obtained from Eq. (2.17) for $n = 0$ and $n = 1$:

$$\nabla_{\hat{\alpha}} N^{\hat{\alpha}} = 0, \qquad \nabla_{\hat{\beta}} T^{\hat{\alpha}\hat{\beta}} = 0. \tag{2.19}$$

The right-hand sides of the above equations vanish since 1 and $p^{\hat{\alpha}}$ are collision invariants [6], i.e.

$$\int \frac{d^3 p}{p^{\hat{0}}} C[f] = \int \frac{d^3 p}{p^{\hat{0}}} C[f] p^{\hat{\alpha}} = 0. \tag{2.20}$$

C. Thermodynamic equilibrium

At local equilibrium, the collision integral $C[f]$ vanishes and f is given by [6,30]

$$f^{(\mathrm{eq})} = \frac{Z}{(2\pi)^3} [\exp(-\beta\mu - \beta p^{\hat{\alpha}} u_{\hat{\alpha}}) - \varepsilon]^{-1}, \tag{2.21}$$

where Z represents the number of degrees of freedom, $\beta = 1/T$ is the inverse local temperature, $u_{\hat{\alpha}}$ are the covariant components of the macroscopic velocity 4-vector, and μ is the chemical potential. The constant ε takes the values -1, 0 and 1 for the Fermi-Dirac (F-D), Maxwell-Jüttner (M-J) and Bose-Einstein (B-E) distributions, respectively. Since the equilibrium distributions corresponding to the F-D or B-E statistics can be inferred from the M-J distribution [17,31], the focus in this paper will be on the latter distribution, which we give explicitly below:

$$f^{(\mathrm{eq})} = \frac{Z}{(2\pi)^3} \exp(\beta\mu + \beta p^{\hat{\alpha}} u_{\hat{\alpha}}). \tag{2.22}$$

When the fluid is in global thermodynamic equilibrium, $f = f^{(\mathrm{eq})}$ everywhere in the spacetime. Substituting Eq. (2.22) into the Boltzmann equation in conservative form (2.16) shows that $\beta\mu$ must be constant, while the vector field $k^{\hat{\alpha}} = \beta u^{\hat{\alpha}}$ must satisfy the Killing equation [6,32–35]:

$$\nabla_{\hat{\alpha}} (\beta\mu) = 0, \qquad k_{\hat{\alpha};\hat{\beta}} + k_{\hat{\beta};\hat{\alpha}} = 0, \tag{2.23}$$

where the semicolon denotes the covariant differentiation. In Sec. III, Eq. (2.23) will be solved for the case of rigidly rotating thermal distributions on general static spherically symmetric spacetimes.

D. Transport coefficients

1. Out-of-equilibrium flows

In an out-of-equilibrium flow, the distribution function f is generally different from $f^{(\mathrm{eq})}$. In the Eckart decomposition, the particle flow 4-vector $N^{\hat{\alpha}} \equiv T^{\hat{\alpha}}$ and the stress-energy tensor $T^{\hat{\alpha}\hat{\beta}}$, corresponding to the cases $n = 0$ and $n = 1$ in Eq. (2.18), respectively, can be written as [6,27,36]

$$N^{\hat{\alpha}} = n u^{\hat{\alpha}}, \tag{2.24a}$$

$$T^{\hat{\alpha}\hat{\beta}} = E u^{\hat{\alpha}} u^{\hat{\beta}} + (P + \overline{\omega}) \Delta^{\hat{\alpha}\hat{\beta}} + 2 q^{(\hat{\alpha}} u^{\hat{\beta})} + \pi^{\hat{\alpha}\hat{\beta}}, \tag{2.24b}$$

where the energy density E and hydrostatic pressure P define the nonequilibrium inverse temperature β through Eq. (C5). The energy density E, dynamic pressure $\overline{\omega}$, heat flux $q^{\hat{\alpha}}$ and pressure deviator $\pi^{\hat{\alpha}\hat{\beta}}$ can be computed from $T^{\hat{\alpha}\hat{\beta}}$ using the following expressions:

$$E = u_{\hat{\alpha}} u_{\hat{\beta}} T^{\hat{\alpha}\hat{\beta}}, \tag{2.25a}$$

$$P + \overline{\omega} = \frac{1}{3} \Delta_{\hat{\alpha}\hat{\beta}} T^{\hat{\alpha}\hat{\beta}}, \tag{2.25b}$$

$$q^{\hat{\alpha}} = -\Delta^{\hat{\alpha}}{}_{\hat{\beta}} u_{\hat{\gamma}} T^{\hat{\beta}\hat{\gamma}}, \tag{2.25c}$$

$$\pi^{\hat{\alpha}\hat{\beta}} = T^{\langle \hat{\alpha}\hat{\beta} \rangle}, \tag{2.25d}$$

where the notation $A^{\langle\hat{\alpha}\hat{\beta}\rangle}$ refers to

$$A^{\langle\hat{\alpha}\hat{\beta}\rangle} \equiv \left[\frac{1}{2}(\Delta^{\hat{\alpha}}{}_{\hat{\gamma}}\Delta^{\hat{\beta}}{}_{\hat{\rho}} + \Delta^{\hat{\alpha}}{}_{\hat{\rho}}\Delta^{\hat{\beta}}{}_{\hat{\gamma}}) - \frac{1}{3}\Delta^{\hat{\alpha}\hat{\beta}}\Delta_{\hat{\gamma}\hat{\rho}}\right]A^{\hat{\gamma}\hat{\rho}}. \quad (2.26)$$

In the hydrodynamic limit, the following relations hold [6,27]:

$$\overline{\omega} = -\eta\nabla_{\hat{\gamma}}u^{\hat{\gamma}}, \quad (2.27a)$$

$$q^{\hat{\alpha}} = -\lambda\Delta^{\hat{\alpha}\hat{\beta}}\left(\nabla_{\hat{\beta}}T - \frac{T}{E+P}\nabla_{\hat{\beta}}P\right), \quad (2.27b)$$

$$\pi_{\hat{\alpha}\hat{\beta}} = -2\mu\nabla_{\langle\hat{\alpha}}u_{\hat{\beta}\rangle}, \quad (2.27c)$$

where $T = \beta^{-1}$ and the bulk viscosity η, shear viscosity μ and thermal conductivity λ are the transport coefficients which make the subject of the present subsection.

2. Transport coefficients in the Marle model

The values of the transport coefficients depend on the form of the collision operator $C[f]$ in the Boltzmann equation (2.16). In general, $C[f]$ is a nonlinear integral operator which drives f towards local thermodynamical equilibrium [6,37]. The computation of the transport coefficients requires the analysis of the hydrodynamic regime of the Boltzmann equation, for the recovery of which there are various procedures, including the Chapman-Enskog procedure [20,38], the Grad moments method [6] and the renormalization group method [39–41]. To illustrate the methodology for the computation of the transport coefficients, we employ in this section the single relaxation time models proposed by Marle [20] and Anderson-Witting [42]:

$$C[f]_{\mathrm{M}} = -\frac{m}{\tau}(f - f^{(\mathrm{eq})}), \quad (2.28a)$$

$$C[f]_{\mathrm{A-W}} = \frac{u_{\hat{\alpha}}p^{\hat{\alpha}}}{\tau}(f - f^{(\mathrm{eq})}), \quad (2.28b)$$

where τ is the relaxation time. For the remainder of this section, we only consider the Marle collision term, with which the Boltzmann equation (2.16) in conservative form reads

$$\frac{1}{\sqrt{-g}}\partial_{\mu}(\sqrt{-g}p^{\hat{\alpha}}e^{\mu}_{\hat{\alpha}}f) - p^{\hat{0}}\frac{\partial}{\partial p^{\hat{i}}}\left(\Gamma^{\hat{i}}{}_{\hat{\alpha}\hat{\beta}}\frac{p^{\hat{\alpha}}p^{\hat{\beta}}}{p^{\hat{0}}}f\right) = -\frac{m}{\tau}(f - f^{(\mathrm{eq})}). \quad (2.29)$$

In order for the Marle model (2.28a) to be consistent, the collision invariants 1 and $p^{\hat{\alpha}}$ must be preserved. Replacing Eq. (2.28a) in Eq. (2.20) gives

$$\nabla_{\hat{\alpha}}N^{\hat{\alpha}} = -\frac{m}{\tau}\int\frac{d^3p}{p^{\hat{0}}}(f - f^{(\mathrm{eq})}) = \frac{1}{m\tau}(T^{\hat{\alpha}}{}_{\hat{\alpha}} - T_E^{\hat{\alpha}}{}_{\hat{\alpha}}), \quad (2.30a)$$

$$\nabla_{\hat{\beta}}T^{\hat{\alpha}\hat{\beta}} = -\frac{m}{\tau}(N^{\hat{\alpha}} - N_E^{\hat{\alpha}}). \quad (2.30b)$$

The above equations can be used to determine the parameters n_E, $u_E^{\hat{\alpha}}$ and T_E of the Maxwell-Jüttner distribution $f^{(\mathrm{eq})}$, as well as of the corresponding "equilibrium" stress-energy tensor $T_E^{\hat{\alpha}\hat{\beta}}$. Since $N^{\hat{\alpha}} = nu^{\hat{\alpha}}$ and $N_E^{\hat{\alpha}} = n_E u_E^{\hat{\alpha}}$ by virtue of Eq. (2.24a), the requirement that the right-hand side of Eq. (2.30b) vanishes imposes

$$n_E = n, \qquad u_E^{\hat{\alpha}} = u_{\hat{\alpha}}. \quad (2.31)$$

By contracting Eq. (2.24b), Eq. (2.30a) reduces to

$$E_E - 3P_E = E - 3(P + \overline{\omega}). \quad (2.32)$$

It is important to note that β_E, defined by Eq. (2.32), does not in general coincide with the inverse temperature β of the system, which is defined by Eq. (C5) in terms of the energy density E corresponding to the stress-energy tensor $T^{\hat{\alpha}\hat{\beta}}$ computed from f.

The expressions for the transport coefficients in the hydrodynamic limit (i.e. when f is not far from $f^{(\mathrm{eq})}$) can be obtained using the Chapman-Enskog method. Since the explicit calculation is quite technical, we provide the necessary details in Appendix C, while here we only summarize the final results:

$$\eta = \frac{\tau P_E(3 - c_{v,E})}{3c_{v,E}^2}(20G_E + 3\zeta_E - 3\zeta_E G_E^2 - 2\zeta_E^2 G_E - 10\zeta_E G_E^2 + 2\zeta_E^2 G_E^3), \quad (2.33a)$$

$$\lambda = \frac{\tau P_E}{m}(1 + c_{v;E}), \quad (2.33b)$$

$$\mu = \tau P_E G_E, \quad (2.33c)$$

where $G_E \equiv G(\zeta_E)$ is defined in Eq. (C6) in terms of the relativistic coldness $\zeta_E = m\beta_E$.

3. Relaxation time and effective transport coefficients

According to Ref. [6], the generalization of the relaxation time τ to the relativistic case yields the following expression [38]:

$$\tau = \frac{1}{n\sigma\mathcal{V}}, \quad (2.34)$$

where σ is the cross section and the mean velocity $\mathcal{V}$ can be taken to represent either the average of the Möller velocity

$g_\phi = \sqrt{(\boldsymbol{v}-\boldsymbol{v}_*)^2 - (\boldsymbol{v}\times\boldsymbol{v}_*)^2}$, or of the modulus of the velocity $\boldsymbol{v} = c\boldsymbol{p}/p^{\hat{0}}$:

$$\langle g_\phi\rangle = \frac{2}{\zeta_E^2[K_1(\zeta_E)]^2}[4\zeta_E^2\mathrm{Ki}_2(2\zeta_E) + 6\zeta_E\mathrm{Ki}_3(2\zeta_E) + (3-4\zeta_E^2)\mathrm{Ki}_4(2\zeta_E) - 6\zeta_E\mathrm{Ki}_5(2\zeta_E) - 3\mathrm{Ki}_6(2\zeta_E)], \tag{2.35a}$$

$$\langle v\rangle = \frac{\zeta_E}{K_1(\zeta_E)}\left[e^{-\zeta_E}\frac{1+\zeta_E}{\zeta_E^2} - \Gamma(0,\zeta_E)\right], \tag{2.35b}$$

where $\mathrm{Ki}_n(z)$ is the repeated integral of $K_0(z)$, defined as [6,43,44]

$$\mathrm{Ki}_n(z) = \int_0^\infty \frac{e^{-z\cosh t}}{(\cosh t)^n}dt, \tag{2.36}$$

while $\Gamma(\nu,z)$ denotes the incomplete Gamma function [43,44]:

$$\Gamma(\nu,z) = \int_z^\infty dt e^{-t}t^{\nu-1}. \tag{2.37}$$

In order to have a quantitative estimate of how much $\langle g_\phi\rangle$ and $\langle v\rangle$ differ, Fig. 1 shows their dependency on the relativistic coldness ζ, confirming the following limits:

$$\langle g_\phi\rangle \underset{\zeta\ll 1}{\to} \frac{4}{5}, \qquad \langle g_\phi\rangle \underset{\zeta\gg 1}{\to} \sqrt{\frac{16}{\pi\zeta}}, \tag{2.38a}$$

$$\langle v\rangle \underset{\zeta\ll 1}{\to} 1, \qquad \langle v\rangle \underset{\zeta\gg 1}{\to} \sqrt{\frac{8}{\pi\zeta}}. \tag{2.38b}$$

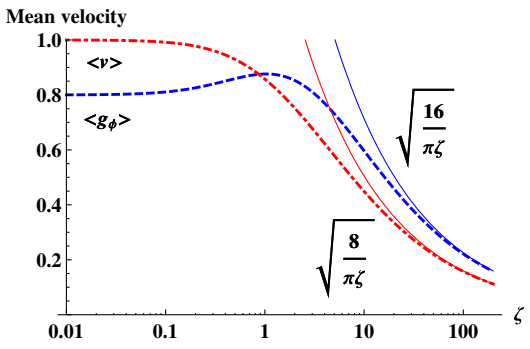

FIG. 1. Comparison between the mean of the Möller velocity $\langle g_\phi\rangle$ (2.35a) and of the modulus of the velocity $\langle v\rangle$ (2.35b) as functions of the relativistic coldness ζ. The limits (2.38) at small and large ζ are confirmed: $\langle g_\phi\rangle$ goes to $\frac{4}{5}$ at small ζ and is well approximated by $\sqrt{16/\pi\zeta}$ at large ζ; while $\langle v\rangle$ goes to 1 (the speed of light) as $\zeta\to 0$, while at large ζ, it behaves like $\sqrt{8/\pi\zeta}$.

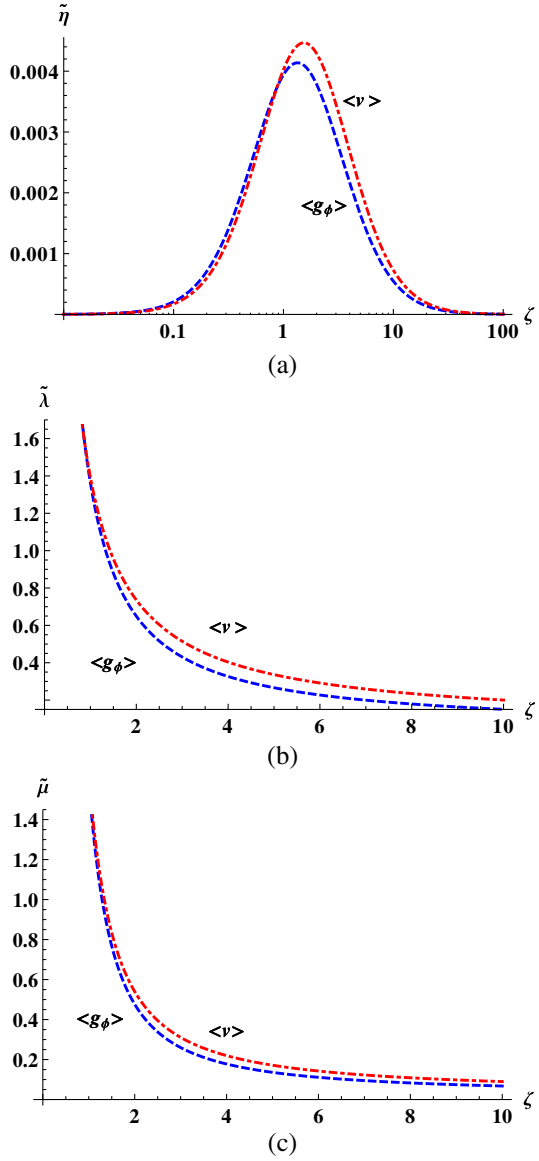

FIG. 2. Plots of (a) the effective bulk viscosity $\tilde{\eta}\equiv a^2\eta/m$; (b) the thermal conductivity $\tilde{\lambda}\equiv a^2\lambda$; and (c) the shear viscosity $\tilde{\mu}\equiv a^2\mu/m$. Each plot shows two curves, corresponding to the cases when the mean velocity in Eq. (2.34) is taken to be the average of the Möller velocity $\langle g_\phi\rangle$ and the average of the particle velocity $\langle v\rangle$, respectively. It can be seen that, in both cases, the coefficient of shear viscosity has a maximum located at $\zeta_{\langle g_\phi\rangle} = 1.342$ and $\zeta_{\langle v\rangle} = 1.535$, having the values $\tilde{\eta}(\zeta_{\langle g_\phi\rangle}) = 3.292\times 10^{-4}$ and $\tilde{\eta}(\zeta_{\langle v\rangle}) = 3.554\times 10^{-4}$, respectively.

It is also interesting to note that the maximum value of $\langle g_\phi\rangle$ is attained at $\zeta_{\max}\simeq 1.034$, where $\langle g_\phi\rangle\simeq 0.876$.

Using Eq. (2.34) for the definition of τ, it is convenient to introduce the following notation:

$$\tilde{\eta} = \frac{\sigma\eta}{m}, \qquad \tilde{\lambda} = \sigma\lambda, \qquad \tilde{\mu} = \frac{\sigma\mu}{m}, \tag{2.39}$$

where the "effective" transport coefficients $\tilde{\eta}$, $\tilde{\lambda}$ and $\tilde{\mu}$ only depend on ζ_E (since $P_E = nm/\zeta_E$). Figure 2 shows a comparison of Eq. (2.39) in terms of ζ when the mean velocity is taken to be $\langle g_\phi \rangle$ or $\langle v \rangle$. It can be seen that, while $\tilde{\lambda}$ and $\tilde{\mu}$ decrease monotonically from infinite values at $\zeta \to 0$ to 0 as $\zeta \to \infty$, the "effective" bulk viscosity $\tilde{\eta}$ presents a maximum value at $\zeta = \zeta_{\max}$, while decreasing to 0 as $\zeta \to 0$ or $\zeta \to \infty$. The value of $\zeta_{\max}$ depends on the definition of the mean velocity, having the value $\zeta_{\langle g_\phi \rangle} = 1.342$ and $\zeta_{\langle v \rangle} = 1.535$, when the mean velocity is taken as $\langle g_\phi \rangle$ and $\langle v \rangle$, respectively. A direct comparison of the curves for the transport coefficients corresponding to the relaxation time constructed using $\langle g_\phi \rangle$ and $\langle v \rangle$ reveals that their qualitative behavior is the same. Thus, for the remainder of this paper, we will only discuss the case when $\langle v \rangle$ is employed.

To conclude this section, it is worth emphasizing that the tetrad formalism has made possible the analogy between the computation of the transport coefficients on curved spaces with respect to arbitrary coordinate systems and on Minkowski space in Cartesian coordinates, as discussed in Appendix C. Moreover, the expressions (2.33) for the coefficients of bulk viscosity, thermal conductivity and shear viscosity are identical to those obtained for Minkowski space [6], in agreement with Einstein's equivalence principle. This is not surprising, since the equations (2.27) defining the transport coefficients, as well as Eq. (C12) describing the nonequilibrium part of the stress-energy tensor, are written in a covariant form, reducing to the Minkowski expressions presented in Ref. [6] in the flat-space limit. The effect of curvature is however felt through the covariant derivatives in Eqs. (2.27), which define the transport coefficients. It is worth writing down the expression for $\nabla_{\hat{\gamma}} u^{\hat{\gamma}}$ appearing in Eq. (2.27a):

$$\nabla_{\hat{\gamma}} u^{\hat{\gamma}} = e^{\mu}_{\hat{\gamma}} \partial_\mu u^{\hat{\gamma}} + \Gamma^{\hat{\gamma}}{}_{\hat{\beta}\hat{\gamma}} u^{\hat{\beta}} = \Gamma^{\hat{\gamma}}{}_{\hat{0}\hat{\gamma}}, \tag{2.40}$$

since, in the comoving frame, $u^{\hat{\gamma}} = (1, 0, 0, 0)$.

Finally, we note that the expressions that we obtained for the transport coefficients depend on the form of the constitutive equations. In this section, we defined the transport coefficients using Eqs. (2.27), which represent the covariant form of the standard definitions on Minkowski space [27]. While other definitions of the transport coefficients are possible [25,26], in this paper we only consider the covariant formalism presented in this section.

III. ROTATING FLOWS IN CENTRAL CHARTS

In this section, we consider an application of the formalism presented in Sec. II to the case of flows undergoing rigid rotation on spherically symmetric spacetimes. In Sec. III A, the expression of the inverse temperature β and 4-velocity u^μ are found by solving the Killing equation (2.23). Section III B defines the comoving frame using the Lorentz boost (2.8) introduced in Sec. II A. Section III C ends this section with a discussion of the form of the rigidly rotating equilibrium states on arbitrary static spherically symmetric spacetimes.

A. Four-velocity

Let us consider a central chart (i.e. static and spherically symmetric) whose metric in spherical coordinates $(x^\mu) = (t, r, \theta, \varphi)$ may be written in the general form

$$ds^2 = w^2 \left[-dt^2 + \frac{dr^2}{u^2} + \frac{r^2}{v^2}(d\theta^2 + \sin^2\theta d\varphi^2) \right], \tag{3.1}$$

where u, v and w depend only on the radial coordinate r. The nonvanishing Christoffel symbols corresponding to the above metric are given below (the prime denotes differentiation with respect to r):

$$\begin{aligned}
&\Gamma^t{}_{tr} = \frac{w'}{w}, \qquad \Gamma^r{}_{tt} = u^2 \frac{w'}{w}, \qquad \Gamma^r{}_{rr} = \frac{w'}{w} - \frac{u'}{u}, \\
&\Gamma^r{}_{\theta\theta} = \frac{u^2 r^2}{v^2}\left(\frac{w'}{w} + \frac{1}{r} - \frac{v'}{v}\right), \qquad \Gamma^\theta{}_{\varphi\varphi} = -\sin\theta\cos\theta \\
&\Gamma^r{}_{\varphi\varphi} = -\frac{u^2\rho^2}{v^2}\left(\frac{w'}{w} + \frac{1}{r} - \frac{v'}{v}\right), \qquad \Gamma^\varphi{}_{\theta\varphi} = \cot\theta, \\
&\Gamma^\theta{}_{r\theta} = \Gamma^\varphi{}_{r\varphi} = \frac{w'}{w} + \frac{1}{r} - \frac{v'}{v}.
\end{aligned} \tag{3.2}$$

For the remainder of this paper, we will consider rigidly rotating flows rotating with constant angular velocity Ω about the z axis. The only nonvanishing components of the 4-velocity of such flows are u^t and u^φ, which can be found once $k^\mu = (k^t, 0, 0, k^\varphi)^T$ is known. Substituting $(\mu, \nu) = (t, r)$ in Eq. (2.23) gives

$$k_t = C_1 w^2(r), \tag{3.3}$$

where C_1 is an integration constant. Furthermore, setting $(\mu, \nu) = (r, \varphi)$ in Eq. (2.23) gives

$$k_\varphi = \Theta(\theta)\left(\frac{wr}{v}\right)^2. \tag{3.4}$$

The function $\Theta(\theta)$ can be determined by setting $(\mu, \nu) = (\theta, \varphi)$:

$$\Theta(\theta) = C_2 \sin^2\theta, \tag{3.5}$$

where C_2 is an integration constant. Let us consider the norm of k^μ:

$$k^2 \equiv g_{\mu\nu} k^\mu k^\nu = -C_1^2 w^2 + C_2^2 \left(\frac{w\rho}{v}\right)^2, \tag{3.6}$$

where $\rho = r\sin\theta$ represents the distance to the z axis. Since $k^2 = -\beta^2$, it is convenient to set $C_1 = -\beta_0$ and $C_2 = \beta_0\Omega$, such that

$$k^\mu = \beta_0(1,0,0,\Omega)^T, \tag{3.7a}$$

$$\beta \equiv \beta(r,\theta) = \beta_0 w\sqrt{1-\left(\frac{\rho\Omega}{v}\right)^2}. \tag{3.7b}$$

The velocity field u^μ can be obtained by dividing k^μ (3.7a) by β (3.7b):

$$u^\mu = \frac{\gamma}{w(r)}(1,0,0,\Omega)^T, \tag{3.8}$$

where the Lorentz factor γ is defined as

$$\gamma = \frac{1}{\sqrt{1-\left(\frac{\rho\Omega}{v}\right)^2}}. \tag{3.9}$$

B. Comoving frame

In this subsection, we follow the steps in Sec. II A in order to define a comoving tetrad for the problem of rigidly rotating flows described in the previous subsection. The first step is to construct a tetrad with respect to which the spacetime metric (3.1) is diagonal. Such a local frame is that of the diagonal gauge, defined as

$$\begin{aligned} e_{\tilde{0}} &= \frac{1}{w}\partial_t, & \omega^{\tilde{0}} &= w dt, \\ e_{\tilde{r}} &= \frac{u}{w}\partial_r, & \omega^{\tilde{r}} &= \frac{w}{u}dr, \\ e_{\tilde{\theta}} &= \frac{v}{rw}\partial_\theta, & \omega^{\tilde{\theta}} &= \frac{rw}{v}d\theta, \\ e_{\tilde{\varphi}} &= \frac{v}{\rho w}\partial_\varphi, & \omega^{\tilde{\varphi}} &= \frac{\rho w}{v}d\varphi. \end{aligned} \tag{3.10}$$

With respect to the above tetrad, the flow four-velocity (3.8) has the following components:

$$u^{\tilde{a}} = \gamma\left(1,0,0,\frac{\rho\Omega}{v}\right)^T, \tag{3.11}$$

where we remind the reader that $\rho = r\sin\theta$ is the distance to the z axis, Ω is the angular velocity of the rotation, the Lorentz factor γ is defined in Eq. (3.9) and $v \equiv v(r)$ is defined in Eq. (3.1). Substituting $u^{\tilde{a}}$ in Eq. (2.8), the following expression can be found for the Lorentz boost $L^{\tilde{a}}{}_{\hat{\alpha}}$:

$$L^{\tilde{a}}{}_{\hat{\alpha}} = \begin{pmatrix} \gamma & 0 & 0 & \frac{\gamma\rho\Omega}{v} \\ 0 & 1 & 0 & 0 \\ 0 & 0 & 1 & 0 \\ \frac{\gamma\rho\Omega}{v} & 0 & 0 & \gamma \end{pmatrix}. \tag{3.12}$$

The comoving frame vectors can now be calculated:

$$\begin{aligned} e_{\hat{0}} &= \frac{\gamma}{w}(\partial_t + \Omega\partial_\varphi), \\ e_{\hat{r}} &= \frac{u}{w}\partial_r, \\ e_{\hat{\theta}} &= \frac{v}{rw}\partial_\theta, \\ e_{\hat{\varphi}} &= \frac{\gamma}{w}\left(\frac{\rho\Omega}{v}\partial_t + \frac{v}{\rho}\partial_\varphi\right). \end{aligned} \tag{3.13}$$

while the corresponding coframe one-forms are given by

$$\begin{aligned} \omega^{\hat{0}} &= \gamma w\left(dt - \frac{\rho^2\Omega}{v^2}d\varphi\right), \\ \omega^{\hat{r}} &= \frac{w}{u}dr, \\ \omega^{\hat{\theta}} &= \frac{rw}{v}d\theta, \\ \omega^{\hat{\varphi}} &= \frac{\rho\gamma w}{v}(-\Omega dt + d\varphi). \end{aligned} \tag{3.14}$$

The expression for $L^{\hat{\alpha}}{}_{\tilde{a}}$ is useful in obtaining the above coframe one-forms:

$$L^{\hat{\alpha}}{}_{\tilde{a}} = \begin{pmatrix} \gamma & 0 & 0 & -\frac{\gamma\rho\Omega}{v} \\ 0 & 1 & 0 & 0 \\ 0 & 0 & 1 & 0 \\ -\frac{\gamma\rho\Omega}{v} & 0 & 0 & \gamma \end{pmatrix}. \tag{3.15}$$

It is now easy to check that the spatial components of the flow four-velocity (3.8) vanish with respect to the comoving frame:

$$u^{\hat{\alpha}} = (1,0,0,0)^T. \tag{3.16}$$

Before ending this section, it is worth giving the metric (3.1) with respect to corotating coordinates, defined as $t = t_{\text{static}}$ and $\varphi = \varphi_{\text{static}} - \Omega t_{\text{static}}$:

$$ds^2 = w^2\left[-\gamma^{-2}dt^2 + \frac{2\rho^2\Omega}{v^2}dtd\varphi + \frac{dr^2}{u^2} + \frac{r^2}{v^2}d\Omega^2\right]. \tag{3.17}$$

Thus, the corotating observer sees $g_{00} \to 0$ as the Killing horizon (i.e. where $k^\mu = u\beta^\mu$ becomes null) is approached:

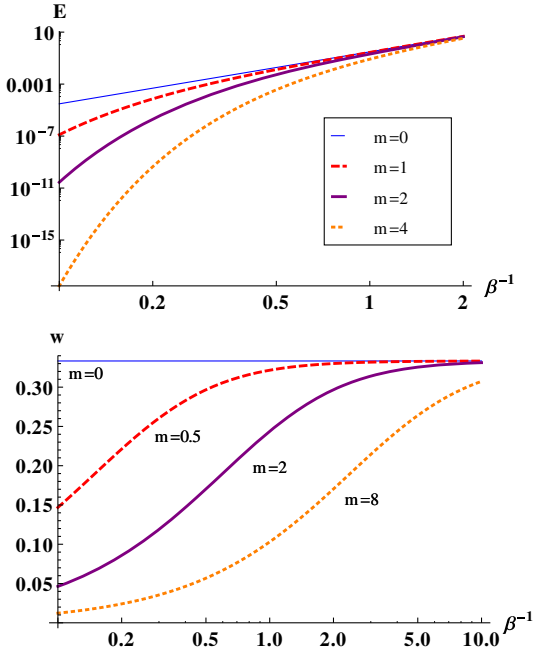

FIG. 3. The dependence of the energy density E (top) and equation of state $w = P/E$ (bottom) on the inverse temperature β^{-1}, for various values of the mass m. The expressions for E and P can be found in Eqs. (3.21a) and (3.21b), respectively.

$$-g_{00} = w^2\left(1 - \frac{\rho^2\Omega^2}{v^2}\right) = \frac{\beta^2}{\beta_0^2} = 0. \tag{3.18}$$

It can be seen that, on these Killing horizons, the temperature β^{-1} tends to infinity, in agreement with Tolman's law [45,46]. In Sec. IV, we will discuss the structure of these horizons for the particular cases of maximally symmetric spacetimes and of the Schwarzschild and Reissner-Nordström (charged) black holes.

C. Equilibrium states

According to the first of Eqs. (2.23), the chemical potential for a state in global thermodynamic equilibrium is constant. Setting, without loss of generality, the chemical potential to 0, the Maxwell-Jüttner (M-J) distribution function (2.22) can be written with respect to the tetrad field $\{e_{\hat{\alpha}}\}$ (when $p_\mu u^\mu = -p^{\hat{0}}$) as follows:

$$f^{(\mathrm{eq})} \equiv f^{(\mathrm{eq})}(Z;\beta) = \frac{Z}{(2\pi)^3} e^{-\beta p^{\hat{0}}}, \tag{3.19}$$

giving rise to the following macroscopic quantities:

$$N^{\hat{\alpha}}_{\mathrm{eq}} = \int \frac{d^3p}{p^{\hat{0}}} f^{(\mathrm{eq})} p^{\hat{\alpha}} = (n,0,0,0)^T, \tag{3.20a}$$

$$T^{\hat{\alpha}\hat{\beta}}_{\mathrm{eq}} = \int \frac{d^3p}{p^{\hat{0}}} f^{(\mathrm{eq})} p^{\hat{\alpha}} p^{\hat{\beta}} = \mathrm{diag}(E,P,P,P). \tag{3.20b}$$

The integrals in the above equations can be performed analytically in terms of modified Bessel functions [6,17,31]:

$$E_{\mathrm{M-J}} = \frac{m^2 Z}{2\pi^2\beta^2}[3K_2(m\beta) + m\beta K_1(m\beta)], \tag{3.21a}$$

$$P_{\mathrm{M-J}} = \frac{m^2 Z}{2\pi^2\beta^2} K_2(m\beta), \tag{3.21b}$$

while $n = \beta P$. While in this paper we only considered particles obeying Maxwell-Jüttner statistics, the above results can readily be extended to Bose-Einstein and Fermi-Dirac statistics, as described in Refs. [17,31].

Since the modified Bessel functions in the expressions of E and P in Eq. (3.21) decrease monotonically as their argument increases, it can be seen that these quantities also decrease monotonically with the increase of m or β. The plots in Fig. 3 show the dependence of the energy density E (3.21a) and equation of state $w = P/E$ with respect to the temperature β^{-1} for various values of the mass, confirming the monotonic behavior of these functions as the temperature is increased.

IV. KILLING HORIZONS FOR RIGIDLY ROTATING STATES

In this section, we consider the properties of rigidly rotating states in global thermodynamic equilibrium. According to Figs. 2 and 3, $\tilde{\lambda}$, $\tilde{\mu}$, E and P (as well as $n = \beta P$) are monotonic functions of β, such that their properties can be inferred directly from the behavior of β. Thus, in this section, only the properties of β and $\tilde{\eta}$ [which has the nontrivial dependence on β depicted in Fig. 2(a)] will be presented.

The analysis of β will be focused on the structure of the Killing horizons seen by corotating observers, as described by Eq. (3.18). Furthermore, the regimes where $\tilde{\eta}$ is monotonic, or where it exhibits regions of local extrema will be discussed. For simplicity, in this section, we only consider the relaxation time (2.34) constructed using $\langle v\rangle$ (2.35b), since the results obtained using $\langle g_\phi\rangle$ are qualitatively similar.

According to Eq. (3.18), the temperature measured by corotating observers diverges on the Killing horizons associated with the Killing vector in Eq. (3.7a). In the case when the metric functions w and v, defined in Eq. (3.1), are nonzero and well defined everywhere in the spacetime, such surfaces represent speed of light surfaces (i.e. where corotating observers travel at the speed of light):

$$1 - \left(\frac{\rho\Omega}{v}\right)^2 = 0. \tag{4.1}$$

The second class refers to horizons which occur in spaces where w and v can vanish for some choice of the spacetime

coordinates. In the absence of rotation, they coincide with the event horizons for the cases of black holes or with the cosmological horizons in the case of the de Sitter expanding universe.

In Sec. IV A, the maximally symmetric spacetimes (e.g. the Minkowski, de Sitter and anti-de Sitter spacetimes) will be discussed. Sections IV B and IV C will be dedicated to the discussion of the properties of the Schwarzschild and Reissner-Nordström spacetimes, respectively.

A. Maximally symmetric spaces

The maximally symmetric spaces which make the subject of the present subsection represent vacuum solutions of the Einstein equations in the presence of a cosmological constant equal to

$$\Lambda = 3\epsilon\omega^2, \tag{4.2}$$

where $\epsilon = 0$, 1 and -1 for the Minkowski, de Sitter and anti-de Sitter spacetimes, respectively. The notation ω refers to the Hubble constant for de Sitter space and to the inverse radius of curvature for anti-de Sitter space. For completeness, we also give the corresponding Ricci scalar:

$$R = 12\epsilon\omega^2. \tag{4.3}$$

The line element can be written as [47]

$$ds^2 = -(1-\epsilon\omega^2 r^2)dt^2 + \frac{dr^2}{1-\epsilon\omega^2 r^2} + r^2 d\Omega^2, \tag{4.4}$$

where the radial coordinate r has the range $[0,\infty)$ on AdS and $r \in [0,\omega^{-1})$ on dS. On dS spacetime, the surface $r = \omega^{-1}$ represents the cosmological horizon. Equation (4.4) can be put in the form of the generic line element in Eq. (3.1) by making the following identifications:

$$w = v = \sqrt{1-\epsilon\omega^2 r^2}, \qquad u = w^2, \tag{4.5}$$

Using Eq. (3.7b), the following expression can be obtained for the inverse temperature β:

$$\beta = \beta_0\sqrt{1-(\epsilon\omega^2 + \Omega^2\sin^2\theta)r^2}, \tag{4.6}$$

where β_0 represents the inverse temperature at the origin $r = 0$. Setting $\Omega = 0$ in Eq. (4.6) shows that, in the absence of rotations, the local temperature β^{-1} remains constant (Minkowski case), decreases to 0 as $r \to \infty$ (AdS case) or increases to infinity as the cosmological horizon $r = \omega^{-1}$ is approached (dS case).

When $\Omega \neq 0$, the rotation induces an SOL where β (4.6) vanishes, such that

$$1 - \epsilon\tilde{r}^2 - \tilde{\rho}^2\tilde{\Omega}^2 = 0, \tag{4.7}$$

where the notation

$$\tilde{r} = \omega r, \qquad \tilde{\rho} = \omega r\sin\theta, \qquad \tilde{\Omega} = \frac{\Omega}{\omega} \tag{4.8}$$

was introduced for convenience. In the case of the Minkowski spacetime ($\epsilon = 0$), the SOL is located where

$$\rho\Omega = 1. \tag{4.9}$$

Rearranging Eq. (4.7) to

$$\tilde{\rho}^2\tilde{\Omega}^2 = 1 - \epsilon\tilde{r}^2 \tag{4.10}$$

shows that the repulsive nature of a positive cosmological constant ($\epsilon = 1$), occurring in the case of the dS space, induces a further centrifugal effect, pulling the SOL inwards with increasing r. In the AdS case ($\epsilon = -1$), the attractive nature of a negative cosmological constant $\Lambda = -3\omega^2$ can play the role of a centripetal force, thus diminishing the effect of rotation.

The position $\tilde{r}_{\rm SOL}$ of the SOL can be found from Eq. (4.7):

$$\tilde{r}_{\rm SOL} = \frac{1}{\sqrt{\tilde{\Omega}^2\sin^2\theta + \epsilon}}. \tag{4.11}$$

On dS, the SOL always forms inside the cosmological horizon, being located at

$$\tilde{r}_{\rm SOL} = \frac{1}{\sqrt{\tilde{\Omega}^2\sin^2\theta + 1}} \quad \text{(de Sitter)}. \tag{4.12}$$

It can be seen that the SOL always touches the cosmological horizon on the rotation axis (i.e. $\sin\theta = 0$), where $\tilde{r}_{\rm SOL} = 1$. This behavior is illustrated in Fig. 4(a).

The situation on AdS is quite different: as shown in Ref. [48], compact manifolds do not exhibit superluminal velocities unless the rotation parameter is sufficiently large. In this case, no SOL forms if $\tilde{\Omega} < 1$ and the temperature β^{-1} remains finite throughout the spacetime. For $\tilde{\Omega} \geq 1$, the location of the SOL is given by

$$\tilde{r}_{\rm SOL} = \frac{1}{\sqrt{\tilde{\Omega}^2\sin^2\theta - 1}} \quad \text{(anti-de Sitter)}, \tag{4.13}$$

where θ is constrained such that $\sin\theta \geq \tilde{\Omega}^{-1}$, as shown in Fig. 4(b). Furthermore, Eq. (4.7) implies that for a fixed value of $\tilde{\Omega}$, the value of β (and indeed of all quantities derived from it, such as n, E, P, $\tilde{\eta}$, $\tilde{\mu}$ and $\tilde{\lambda}$) is constant on the cones having their apex at the origin, for which

$$\sin\theta = \tilde{\Omega}^{-1}. \tag{4.14}$$

In particular, setting $\tilde{\Omega} = 1$ implies that β is constant throughout the equatorial plane.

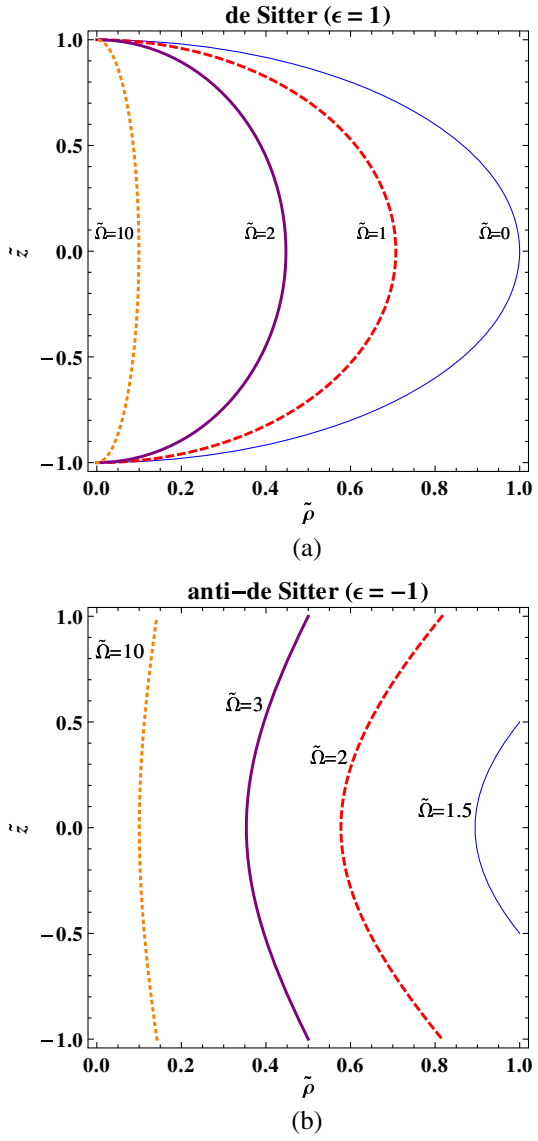

FIG. 4. The SOL structure of (a) dS and (b) AdS. The vertical axis represents the coordinate $\tilde{z} \equiv \omega r \cos\theta$ along the rotation axis, while the horizontal axis represents the distance $\tilde{\rho} \equiv \omega r \sin\theta$ from the rotation axis. In the dS case, the rightmost line corresponding to $\tilde{\Omega} = 0$ represents the cosmological horizon, located at $\tilde{r} = \pi/2$. On AdS, no SOL forms when $\tilde{\Omega} < 1$. The Minkowski case, when $\rho = \tilde{\Omega}^{-1}$, is not shown here.

A more geometric assessment of the location of the SOL is the proper radial distance $\tilde{s} = \omega s$ from the origin to the SOL, which can be written as follows:

$$\tilde{s} = \omega \int_0^{\tilde{r}_{\rm SOL}} d\tilde{r} \sqrt{g_{rr}} = \begin{cases} \arcsin[(\tilde{\Omega}^2 \sin^2\theta + 1)^{-1/2}] & \text{(dS)}, \\ \tilde{\Omega}^{-1} & \text{(Minkowski)}, \\ \operatorname{arcsinh}[(\tilde{\Omega}^2 \sin^2\theta - 1)^{-1/2}] & \text{(AdS)}. \end{cases} \quad (4.15)$$

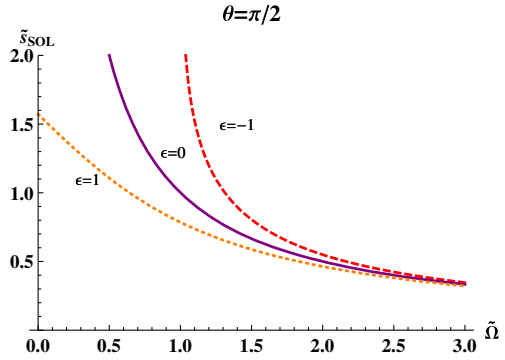

FIG. 5. The proper radial distance $\tilde{s}_{\rm SOL}$ (4.15) between the origin and the SOL in the equatorial plane ($\sin\theta = 1$) with respect to $\tilde{\Omega} = \Omega/\omega$. The bottom, middle and top lines correspond to the cases $\epsilon = 1$ (dS), $\epsilon = 0$ (Minkowski) and $\epsilon = -1$ (AdS). In the case of Minkowski spacetime, we adopt the convention $\tilde{s} = s = \Omega^{-1}$ and $\tilde{\Omega} = \Omega$ (i.e. the parameter ω is immaterial in this case).

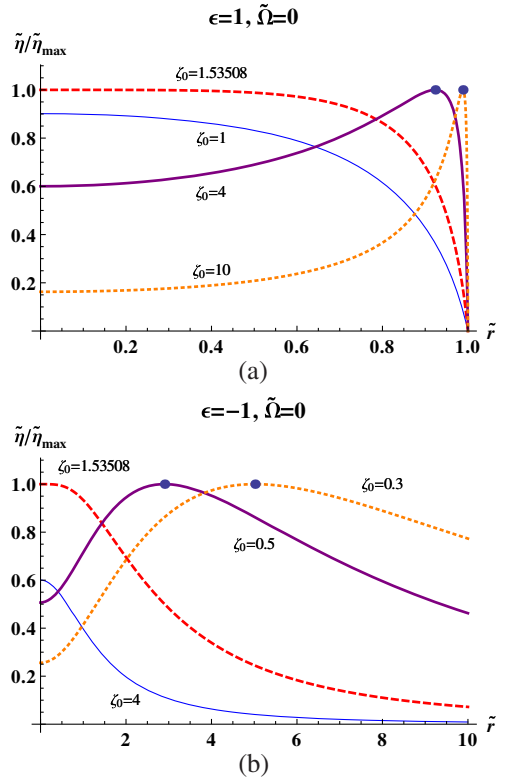

FIG. 6. Dependence of the effective coefficient of bulk viscosity $\tilde{\eta}$ (2.33a) divided by its maximum value $\tilde{\eta}_{\rm max}$ on $\tilde{r}$ on (a) dS and (b) AdS spacetimes in the absence of rotation ($\tilde{\Omega} = 0$). Each curve corresponds to a different value of $\zeta_0 = m\beta_0$, where $\beta_0 \equiv \beta(r = 0)$ is the inverse temperature at the coordinate origin. The local maxima exhibited by $\tilde{\eta}$ (highlighted by circular points) appear only when ζ_0 is large (dS) or small (adS), its locations being given by Eqs. (4.16) and (4.17) for the dS and adS spaces, respectively.

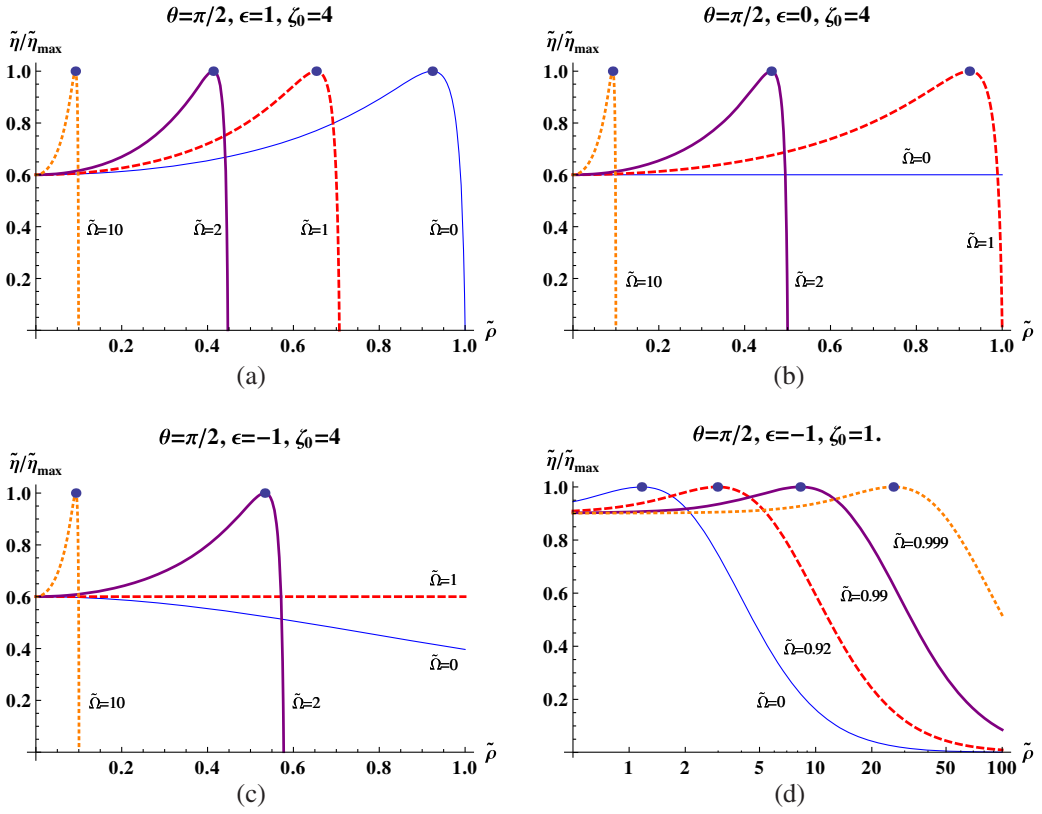

FIG. 7. Dependence of the effective coefficient of bulk viscosity $\tilde{\eta}$ (2.33a) in the equatorial plane ($\theta = \pi/2$) divided by its maximum value $\tilde{\eta}_{\max}$ on (a) dS, (b) Minkowski and (c), (d) AdS spacetimes. Each curve corresponds to a different value of $\tilde{\Omega}$, while the parameter $\zeta_0 = 4$ for (a)–(c) and $\zeta_0 = 1$ for (d). It should be noted that when $\tilde{\Omega} = 1$, $\tilde{\eta}$ is constant in the equatorial plane of AdS space, cf. (4.14).

Figure 5 shows that, for fixed $\tilde{\Omega}$, the distance from the SOL to the rotation axis in the equatorial plane is larger in the AdS and smaller in the dS cases with respect to the same distance in Minkowski space.

The plots in Fig. 6 show the dependence of $\tilde{\eta}$ on $\tilde{r}$ for various values of the relativistic coldness $\zeta_0 = m\beta_0 \equiv m\beta(r=0)$ measured at the origin when $\tilde{\Omega} = 0$ for the cases of (a) the dS and (b) the adS spaces. On dS space, β decreases monotonically from the maximum value β_0 at the origin towards 0 on the cosmological horizon (where $\tilde{r} = 1$). For all $\zeta \le \zeta_{\max} \simeq 1.53508$, Fig. 2(a) implies that $\tilde{\eta}$ also decreases monotonically, since in this regime, $\tilde{\eta}$ shows no local extrema. However, for all $\zeta_0 > \zeta_{\max}$, $\tilde{\eta}$ increases up to the maximum value $\tilde{\eta}_{\max} \simeq 3.554 \times 10^{-4}$, attained when

$$\tilde{r}_{\max} = \sqrt{1 - \left(\frac{\zeta_{\max}}{\zeta_0}\right)^2}, \tag{4.16}$$

as can be seen in Fig. 6(a). On adS space, ζ increases monotonically from ζ_0 at the origin to infinity as $\tilde{r} \to \infty$. Figure 6(b) shows that $\tilde{\eta}$ also decreases monotonically to 0 as $\tilde{r} \to \infty$ for all $\zeta_0 \ge \zeta_{\max}$, while in the case when $\zeta_0 < \zeta_{\max}$, $\tilde{\eta}$ attains the maximum value $\tilde{\eta}_{\max}$ when

$$\tilde{r}_{\max} = \sqrt{\left(\frac{\zeta_{\max}}{\zeta_0}\right)^2 - 1}. \tag{4.17}$$

At nonvanishing values of $\tilde{\Omega}$, $\tilde{\eta}$ attains the maximum value $\tilde{\eta}_{\max}$ at

$$\tilde{r}_{\max} = \left[\frac{1 - (\zeta_{\max}/\zeta_0)^2}{\tilde{\Omega}^2 + \epsilon}\right]^{1/2}. \tag{4.18}$$

For the dS space, Fig. 7(a) shows that increasing the value of $\tilde{\Omega}$ decreases the distance to the horizon, while the location of the maximum also decreases according to

$$\tilde{r}_{\max}\rfloor_{\mathrm{dS}} = \frac{1}{\sqrt{1+\tilde{\Omega}^2}}\sqrt{1 - \left(\frac{\zeta_{\max}}{\zeta_0}\right)^2}. \tag{4.19}$$

Figure 7(b) shows that, on Minkowski space, $\tilde{\eta}$ is constant throughout the spacetime in the absence of rotation, while for nonvanishing values of $\tilde{\Omega}$, it attains a maximum for all $\zeta_0 \ge \zeta_{\max}$ located at

$$\tilde{r}_{\max}\rfloor_{\mathrm{Mink}} = \frac{1}{\tilde{\Omega}}\sqrt{1 - \left(\frac{\zeta_{\max}}{\zeta_0}\right)^2}. \tag{4.20}$$

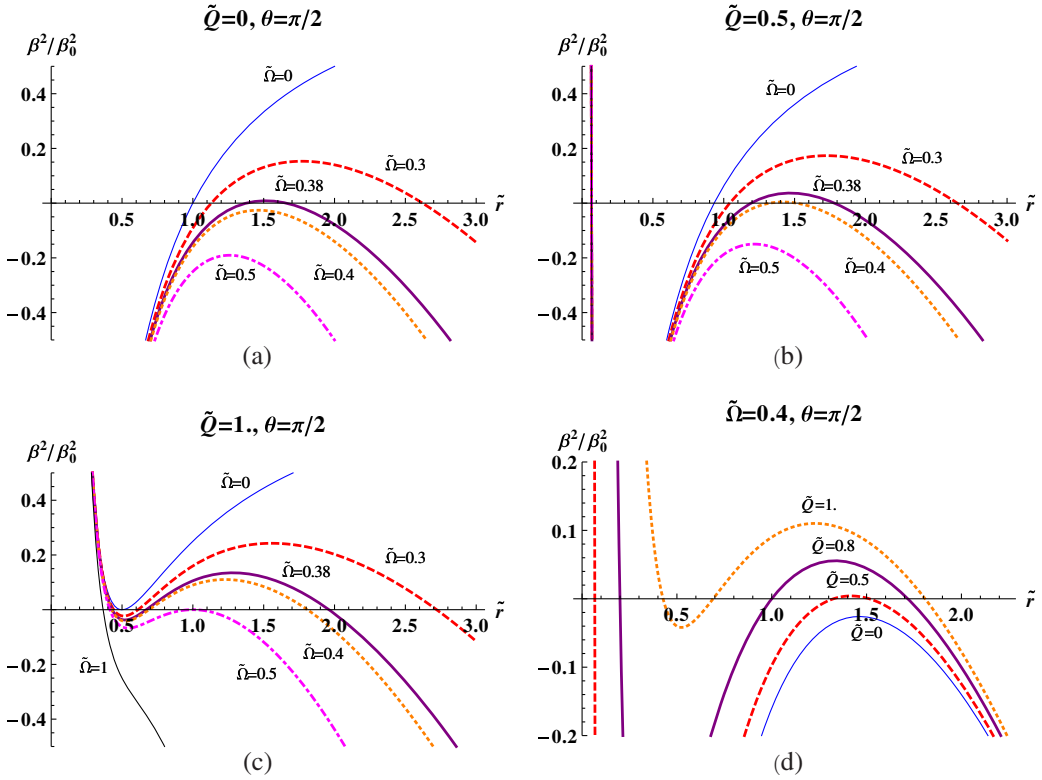

FIG. 8. The dependence of β^2/β_0^2 on $\tilde{r} = r/2M$ in the equatorial plane $\sin\theta = 1$ for (a)-(c) $\tilde{Q}$ fixed at (a) 0 (Schwarzschild space), (b) 0.5 and (c) 1.0 (extremal Reissner-Nordström space), for various values of $\tilde{\Omega} = 2M\Omega$. In (d), $\tilde{\Omega}$ is fixed at 0.4 and the charge is varied from $\tilde{Q} = 0$ to $\tilde{Q} = 1.0$. The regions where $\beta^2 > 0$ represent "allowed" regions (where the temperature is finite and well defined), while the points where $\beta = 0$ represent horizons.

On AdS space, three regimes can be distinguished. When $\tilde{\Omega} > 1$, an SOL forms and the characteristics of $\tilde{\eta}$ are similar to the case when dS space is considered. When $\tilde{\Omega} = 1$, $\tilde{\eta}$ is constant throughout the equatorial plane, as implied by Eq. (4.14). These two regimes can be clearly seen in Fig. 7(c). Finally, when $\tilde{\Omega} < 1$, no SOL forms and $\tilde{\eta}$ only attains a maximum when $\zeta_0 < \zeta_{\max}$, as shown in Fig. 7(d). The coordinate of this maximum increases as $\tilde{\Omega}$ increases.

B. Schwarzschild black hole spacetime

The line element of the Schwarzschild spacetime is given by

$$ds^2 = -\left(1 - \frac{2M}{r}\right)dt^2 + \frac{dr^2}{1 - \frac{2M}{r}} + r^2 d\Omega^2, \tag{4.21}$$

describing the gravitational field of a black hole of mass M. Comparing Eq. (4.21) with Eq. (3.1) gives the following expressions for the metric functions:

$$w = v = \sqrt{1 - \frac{2M}{r}}, \qquad u = 1 - \frac{2M}{r}, \tag{4.22}$$

such that the inverse temperature β (3.7b) becomes

$$\beta = \beta_0 \sqrt{1 - \frac{2M}{r} - \rho^2\Omega^2}, \tag{4.23}$$

where β_0 is the inverse temperature at infinity on the rotation axis (i.e. $z = r\cos\theta \to \pm\infty$ and $\rho = 0$). In the absence of rotation, the temperature β^{-1} increases from β_0 at infinity to an infinite value as the black hole horizon is approached (i.e. $r \to M$). To better investigate the topology of the horizon structure when $\Omega > 0$, it is convenient to cast the equation $\beta^2 = 0$ as

$$\frac{\beta^2}{\beta_0^2} = 1 - \frac{1}{\tilde{r}} - \tilde{\rho}^2\tilde{\Omega}^2 = 0, \tag{4.24}$$

where the following notations were introduced:

$$\tilde{r} = \frac{r}{2M}, \qquad \tilde{\Omega} = 2M\Omega. \tag{4.25}$$

Figure 8(a) shows the dependence of β^2/β_0^2 (4.24) on $\tilde{r}$ in the equatorial plane $\sin\theta = 1$ at various values of $\tilde{\Omega}$ (the rest of the plots in this figure refer to the case of Reissner-Nordström black holes, which are discussed in the following subsection). In the regions where $\beta^2 > 0$, the local temperature β^{-1} is finite and the hydrodynamic moments (3.21) are

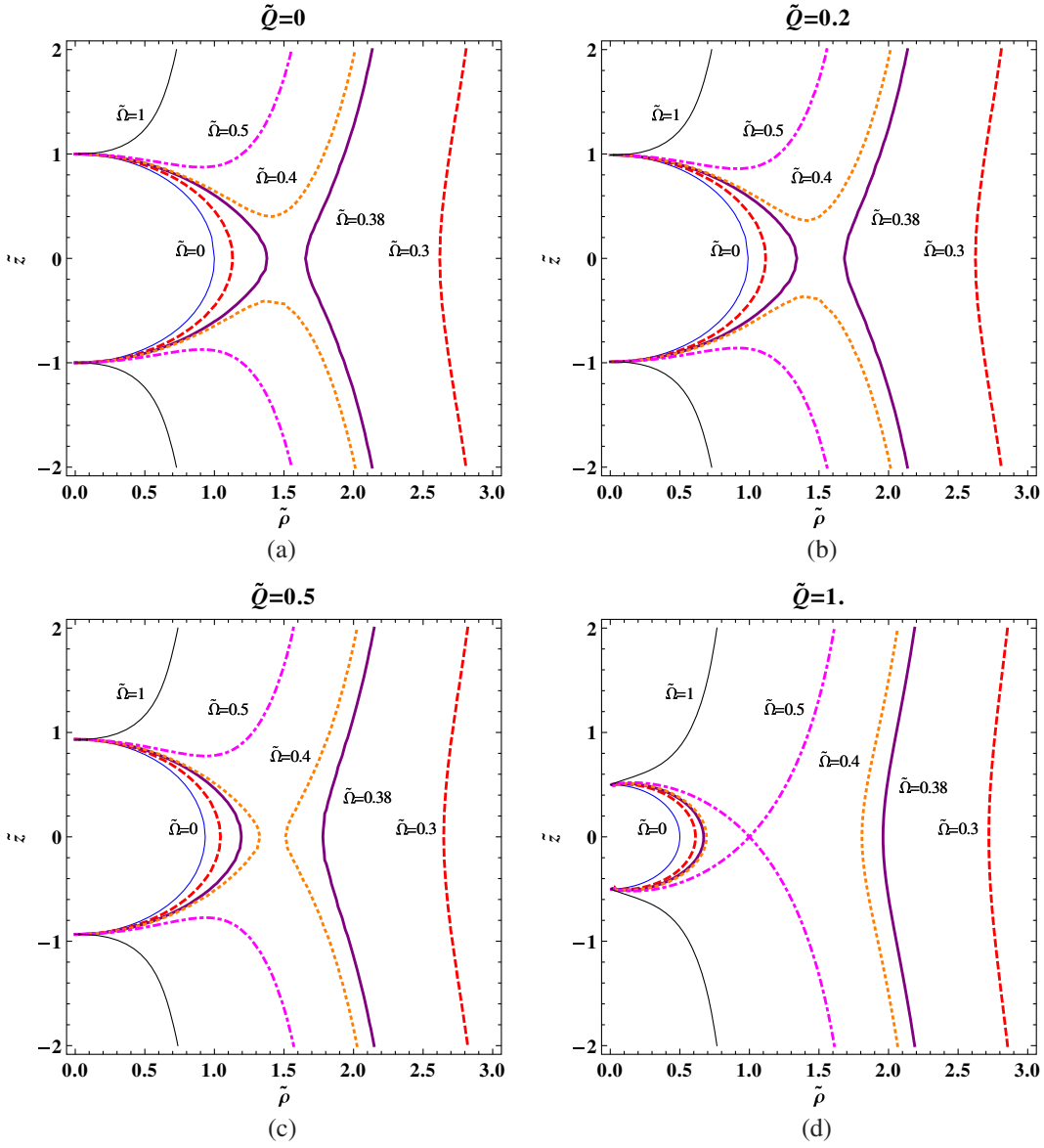

FIG. 9. The SOL structure of the Reissner-Nordström spacetime for four values of $\tilde{Q} = Q/M$. The vertical axis represents the coordinate $\tilde{z} \equiv z/2M$ along the rotation axis, while the horizontal axis represents the distance $\tilde{\rho} = r\sin\theta/2M$ from the rotation axis. The contours represent the surfaces where $\beta = 0$, i.e. either the black hole horizon (only the outer horizons are shown) or the rotation horizon (i.e. where the SOL induced by the rotation forms). The case (a) shows the horizon structure for the Schwarzschild space ($Q = 0$), while the case (d) represents an extremal Reissner-Nordström black hole ($Q = M$).

well defined. At small enough values of $\tilde{\Omega}$, the two intersections of the graph of β^2/β_0^2 with the horizontal axis correspond to the locations of the black hole horizon and of the SOL. As $\tilde{\Omega}$ increases, β^2 remains negative for all values of $\tilde{r}$, showing that the SOL and the black hole event horizon join, forming an exclusion region which incorporates the whole equatorial plane. It is interesting to note that the black hole horizon moves outwards as $\tilde{\Omega}$ is increased, while the SOL moves inwards, as expected.

The horizon structure of the Schwarzschild spacetime is represented in Fig. 9(a) for various values of $\tilde{\Omega}$ (as before, the remaining plots refer to the case of charged black holes, which are discussed in Sec. IV C). It can be seen that increasing $\tilde{\Omega}$ pushes the black hole horizon outwards, while the SOL is pulled inwards. At large enough $\tilde{\Omega}$, these two horizons merge, thus excluding the entire equatorial plane from the region where $\beta^2 > 0$.

In the absence of rotation, $\zeta = m\beta$ increases monotonically from 0 on the event horizon up to ζ_0 as $r \to \infty$. In this case, the dependence of $\tilde{\eta}$ on r is nonmonotonic only when $\zeta_0 > \zeta_{\max}$, as shown in Fig. 10(a). The points of maxima $\tilde{r}_{\max}$ occurring outside the event horizon are located at

$$\tilde{r}_{\max} = [1 - (\zeta_{\max}/\zeta_0)^2]^{-1}, \tag{4.26}$$

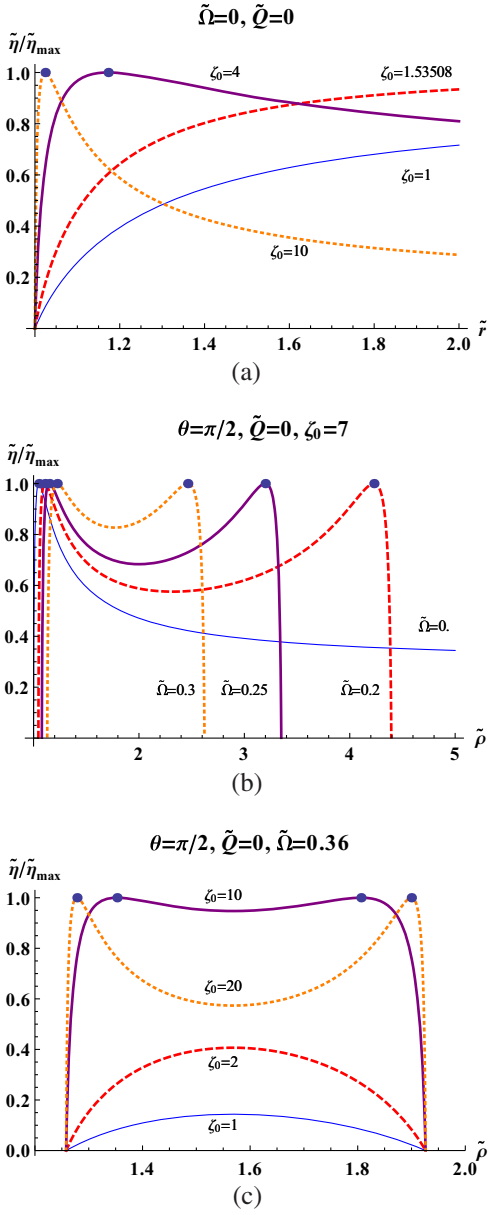

FIG. 10. Dependence of the ratio $\tilde{\eta}/\tilde{\eta}_{\max}$ (2.33a) of the effective coefficient of bulk viscosity divided by its maximum value, evaluated in the equatorial plane ($\theta = \pi/2$), with respect to the distance from the rotation axis for the Schwarzschild space-time ($\tilde{Q} = 0$) in the following cases: (a) $\tilde{\Omega} = 0$ for various values of ζ_0; (b) $\zeta_0 = 7$ for various values of $\tilde{\Omega}$; (c) $\tilde{\Omega} = 0.36$ for various values of ζ_0.

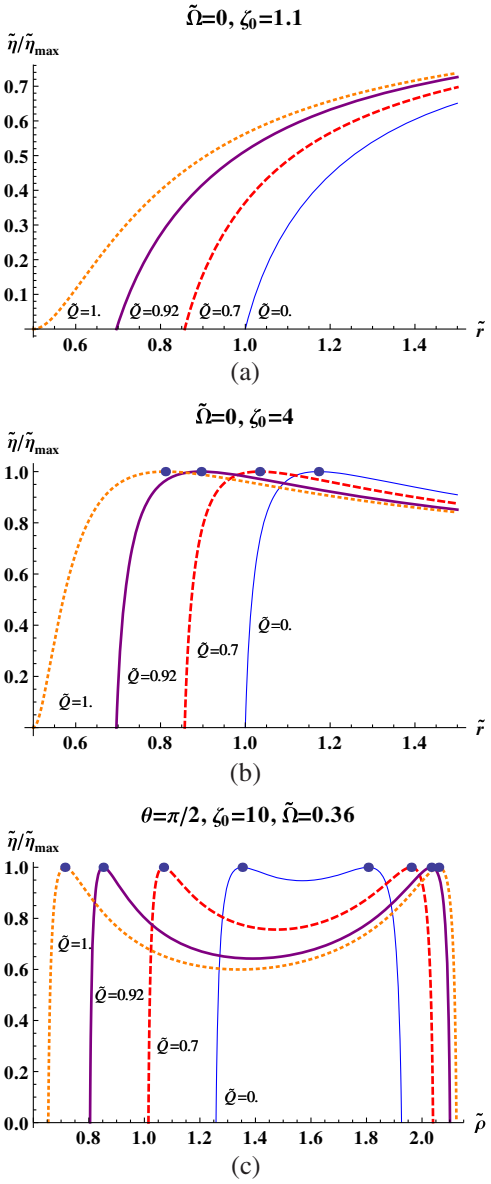

FIG. 11. Same as Fig. 10 for the Reissner-Nordström black hole. (a) $(\tilde{\Omega}, \zeta_0) = (0, 1.1)$; (b) $(\tilde{\Omega}, \zeta_0) = (0, 4)$; (c) $(\tilde{\Omega}, \zeta_0) = (0.36, 10)$, for various values of $\tilde{Q} = Q/M$.

valid only for $\zeta_0 > \zeta_{\max}$. When the rotation is switched on, the location of the points of maxima is given by the following cubic equation:

$$1 - \frac{1}{\tilde{r}} - \tilde{\rho}^2\tilde{\Omega}^2 = \left(\frac{\zeta_{\max}}{\zeta_0}\right)^2. \tag{4.27}$$

Figures 10(b) and 10(c) suggest that $\tilde{\eta}$ can develop two points of maxima with a point of local minimum between the event and rotation horizons. For the cases shown in these plots, it can be seen that the regime where $\tilde{\eta}$ presents a local minimum can be obtained either by increasing $\tilde{\Omega}$ at fixed values of ζ_0, or by increasing ζ_0 at fixed values of $\tilde{\Omega}$. The properties of $\tilde{\eta}$ in the case of the charged black hole are presented in Fig. 11, which is discussed in the following section.

C. Reissner-Nordström metric

Let us now consider the case of a black hole with mass M and charge Q, for which the metric functions in Eq. (4.22) become

$$w = v = \sqrt{1 - \frac{2M}{r} + \frac{Q^2}{r^2}}, \quad u = 1 - \frac{2M}{r} + \frac{Q^2}{r^2}. \tag{4.28}$$

Hence, the inverse temperature β picks up a term which depends on the charge Q, such that Eq. (4.24) becomes

$$\frac{\beta^2}{\beta_0^2} = 1 - \frac{1}{\tilde{r}} + \frac{\tilde{Q}^2}{4\tilde{r}^2} - \tilde{\rho}^2\tilde{\Omega}^2, \tag{4.29}$$

where the reduced charge is defined as $\tilde{Q} = \frac{Q}{M}$. If $\tilde{Q} \neq 0$, the event horizon is split into an inner and an outer horizon, which are located at $\tilde{r}_- = (1 - \sqrt{1 - \tilde{Q}^2})/2$ and $r_+ = (1 + \sqrt{1 - \tilde{Q}^2})/2$, respectively. At $Q = 0$, the inner horizon collapses to the black hole center, while the outer horizon forms at $\tilde{r} = 1$. As Q is increased, the radius of the inner horizon grows, while the outer horizon is pulled in, up to the extremal case $\tilde{Q} = 1$, when the two horizons touch at $\tilde{r}_- = \tilde{r}_+ = 0.5$. While Eq. (4.29) admits up to four roots where β^2 vanishes, some of these solutions may be imaginary, negative or located inside the outer horizon, in which case they will be discarded. In the following, only the roots which correspond to the rotation and the outer horizons will be discussed.

As expected, Figs. 8(b), 8(c) and especially 8(d) confirm that Q acts contrary to M, since as $\tilde{Q}$ is increased at fixed $\tilde{\Omega}$, the outer horizon moves inwards. Furthermore, the SOL is pushed outwards as $\tilde{Q}$ is increased. It is interesting to note that, in the extremal Reissner-Nordström case, an equilibrium distribution of rotating particles sees an event horizon near the black hole which dresses the singularity at $\tilde{r} = 0$. Similar conclusions can be drawn by inspecting the horizon structure presented in Fig. 9.

To assess the effect of $\tilde{Q}$ on $\tilde{\eta}$, the equivalent of Eq. (4.26) when the charge is not zero can be investigated:

$$\tilde{r}_{\max} = \frac{1 + \sqrt{1 - \tilde{Q}^2[1 - (\zeta_{\max}/\zeta_0)^2]}}{2[1 - (\zeta_{\max}/\zeta_0)^2]}. \tag{4.30}$$

As in the case of the Schwarzshild black hole, the above equation also implies that no points of maxima exist unless $\zeta_0 > \zeta_{\max}$. When $\zeta_0 < \zeta_{\max}$ and no maximum of $\tilde{\eta}$ occurs, Fig. 11(a) shows that $\tilde{\eta}$ increases as $\tilde{Q}$ is increased. Furthermore, Fig. 11(b) shows that increasing $\tilde{Q}$ decreases $\tilde{r}_{\max}$ when $\zeta_0 > \zeta_{\max}$. In the rotating case, Eq. (4.27) becomes quartic in $\tilde{r}$:

$$1 - \frac{1}{\tilde{r}} + \frac{\tilde{Q}^2}{4\tilde{r}^2} - \tilde{\rho}^2\tilde{\Omega}^2 = \left(\frac{\zeta_{\max}}{\zeta_0}\right)^2. \tag{4.31}$$

Increasing $\tilde{Q}$ for large enough (fixed) ζ_0 and at fixed $\tilde{\Omega}$ pulls the first maximum towards the rotation axis, while pushing the second maximum towards the SOL, as can be seen from Fig. 11(c).

V. CONCLUSION

In this paper, we employed the tetrad formalism to study the properties of equilibrium states of gases undergoing rigid rotation on spherically symmetric spacetimes. By employing the Boltzmann equation in conservative form [23], we obtained covariant expressions for the transport coefficients when the Marle model for the collision operator is employed. Our results coincide with the expressions on flat spacetime, in agreement with the equivalence principle. In order to study rigidly rotating thermal states, we employed a comoving tetrad field, which we obtained by performing a Lorentz boost on a fixed tetrad which diagonalizes the background spacetime metric. Using the tetrad formalism, we obtained expressions for the particle flow four-vector and stress-energy tensor corresponding to such states. Furthermore, we discussed the formation of speed of light surfaces and their topology in the cases of maximally symmetric spacetimes (Minkowski, anti-de Sitter, and de Sitter spaces) and spherically symmetric black hole spacetimes (i.e. the Schwarzschild and Reissner-Nordström spacetimes).

In constructing the transport coefficients, the Marle model was employed, where the relaxation time was chosen to be inversely proportional to the average of the Möller velocity or the modulus of the velocity. Our analysis showed no qualitative differences between the results obtained using the two aforementioned definitions for the mean velocity. We found that the particle number density, energy density, equilibrium pressure, coefficient of thermal conductivity and coefficient of shear viscosity exhibit a monotonic dependence on the inverse temperature β, such that their properties can be inferred from those of β. However, since the coefficient of bulk viscosity η attains a maximum value at a finite value of β, while decreasing to 0 as β approaches either 0 or infinity, its properties were also studied in detail. We note here that, according to Ref. [49], the Chapman-Enskog analysis indicates that the transport coefficients obtained when the collision term is approximated using the Anderson-Witting model exhibit features which are qualitatively similar to those corresponding to the Marle model. Indeed, the coefficients of thermal conductivity and shear viscosity depend monotonically on β, while the coefficient of bulk viscosity can be approximately related to that obtained in the Marle model by means of a suitable rescaling.

For the case of maximally symmetric spacetimes, we showed that the speed-of-light surface forms closer to the rotation axis on de Sitter space compared to Minkowski space, while on anti-de Sitter space, it forms farther away. Furthermore, no SOL forms on adS if the rotation parameter Ω is smaller than the inverse radius of curvature ω. Our analysis also revealed that, on AdS, the inverse temperature β and all quantities derived from it (i.e. the stress-energy tensor and the transport coefficients) are constant on cones defined by $\Omega \sin\theta = \omega$. In particular, β is constant

throughout the equatorial plane when $\Omega = \omega$. We found that the coefficient of bulk viscosity can display a nonmonotonic behavior for certain values of the relativistic coldness ζ_0 measured at the origin of the spacetime.

In the Schwarzschild case, the SOL plays the role of a "rotational horizon," complementing (and indeed enhancing) the event horizon of the black hole. As the rotation parameter Ω is increased, the distance between the rotational horizon and the rotation axis decreases, while the distance between the event horizon and the rotation axis increases. When the rotation parameter is nonzero, the coefficient of bulk viscosity η can exhibit two points of maxima and one local minimum between the event horizon and the speed-of-light surface.

Similar conclusions were obtained in the case of Reissner-Nordström (charged) black holes. Furthermore, it was shown that increasing the value of the black hole charge at fixed rotation parameter has the inverse effect of decreasing the radius of the event horizon, while pushing the rotational horizon away. In the case of the extremal Reissner-Nordström black hole, the tendency of rotation to close the distance between the event and rotation horizons induces an event horizon which dresses the singularity at the origin. The points of maxima observed in the Schwarzschild case are modified in the same spirit as the Killing horizons, namely the maximum closer to the event horizon is pulled towards the rotation axis, while the maximum farther away is pushed towards the SOL.

We would like to highlight the fact that the results presented in this paper represent a solid starting point for a systematic comparison between kinetic theory results and the properties of rigidly rotating thermal states obtained using quantum field theory on curved spaces. We wish to perform such comparisons for, e.g., rigidly rotating states on the Minkowski spacetime, where analytic results are available from the quantum-field theory approach [14,15], as well as from the kinetic theory approach [17]. Furthermore, similar comparisons can be performed for the case of the anti-de Sitter space, where analytic results obtained using quantum field theory are already available [50]. Another possible extension is in the direction of the Einstein static universe (not covered in the present work), where quantum field theory results for nonrotating thermal states of the Klein-Gordon field were obtained in Ref. [51]. Finally, this work can be extended to the case of rigidly rotating thermal states on axisymmetric spacetimes, such as the Kerr black hole spacetime.

ACKNOWLEDGMENTS

V. E. A. is indebted to Nistor Nicolaevici and Robert Blaga for useful discussions. This work was supported by a grant of the Romanian National Authority for Scientific Research and Innovation, CNCS-UEFISCDI, Project No. PN-II-RU-TE-2014-4-2910.

APPENDIX A: BOLTZMANN EQUATION WITH RESPECT TO NONHOLONOMIC TETRAD FIELDS

In this section of the appendix, the transition from the Boltzmann equation (2.10) with respect to arbitrary coordinates $\{x^\mu\}$ to Eq. (2.13), where nonholonomic tetrad fields are employed, is presented. Following Ref. [6], it is possible to write the exterior derivative of f as follows:

$$\begin{aligned} df &= \left(\frac{\partial f}{\partial x^\mu}\right)_{p^i} dx^\mu + \frac{\partial f}{\partial p^i} dp^i \\ &= \left(\frac{\partial f}{\partial x^\mu}\right)_{p^{\hat{\imath}}} dx^\mu + \frac{\partial f}{\partial p^{\hat{\imath}}} dp^{\hat{\imath}}, \end{aligned} \tag{A1}$$

where on the first line, $\partial f/\partial x^\mu$ is taken while considering p^i to be constant. On the second line, the components $p^{\hat{\imath}} = p^\mu \omega_\mu^{\hat{\imath}}$ with respect to the tetrad one-forms $\{\omega^{\hat{\alpha}}\}$ are kept constant. In order to derive the Boltzmann equation when the components of the momentum 4-vector are expressed with respect to nonholonomic tetrad fields, the derivatives on the first line of Eq. (A1) must be expressed with respect to derivatives on the second line.

Using Eq. (2.11), the following expression can be obtained for the exterior derivative of p^0:

$$dp^0 = -\frac{1}{2} g_{\mu\nu,\lambda} \frac{p^\mu p^\nu}{p_0} dx^\lambda - \frac{p_i}{p_0} dp^i, \tag{A2}$$

such that the exterior derivative of $p^{\hat{\imath}}$ can be written as

$$\begin{aligned} dp^{\hat{\imath}} = &\left(\frac{\partial \omega_\nu^{\hat{\imath}}}{\partial x^\mu} p^\nu - \frac{1}{2} \omega_0^{\hat{\imath}} g_{\alpha\beta,\mu} \frac{p^\alpha p^\beta}{p_0}\right) dx^\mu \\ &+ \left(\omega_j^{\hat{\imath}} - \omega_0^{\hat{\imath}} \frac{p_j}{p_0}\right) dp^j. \end{aligned} \tag{A3}$$

Substituting the above result in Eq. (A1) yields the following identifications:

$$\begin{aligned} \left(\frac{\partial f}{\partial x^\mu}\right)_{p^i} &= \left(\frac{\partial f}{\partial x^\mu}\right)_{p^{\hat{\imath}}} + \frac{\partial f}{\partial p^{\hat{\imath}}} \left(p^\nu \frac{\omega_\nu^{\hat{\imath}}}{\partial x^\mu} - \omega_0^{\hat{\imath}} g_{\alpha\beta,\mu} \frac{p^\alpha p^\beta}{2p_0}\right), \\ \frac{\partial f}{\partial p^i} &= \left(\omega_i^{\hat{\jmath}} - \omega_0^{\hat{\jmath}} \frac{p_i}{p_0}\right) \frac{\partial f}{\partial p^{\hat{\jmath}}}. \end{aligned} \tag{A4}$$

The Boltzmann equation can now be written as

$$\begin{aligned} &p^\mu \left(\frac{\partial f}{\partial x^\mu}\right)_{p^{\hat{\imath}}} - \frac{\partial f}{\partial p^{\hat{\imath}}} \left[-p^\mu p^\nu \frac{\partial \omega_\nu^{\hat{\imath}}}{\partial x^\mu} + \Gamma^j{}_{\mu\nu} p^\mu p^\nu \omega_j^{\hat{\imath}} \right. \\ &\left. - \omega_0^{\hat{\imath}} \left(\Gamma^j{}_{\mu\nu} \frac{p^\mu p^\nu p_i}{p_0} - g_{\alpha\beta,\mu} \frac{p^\alpha p^\beta p^\mu}{2p_0}\right)\right] = C[f]. \end{aligned} \tag{A5}$$

The term involving the derivative of the metric $g_{\alpha\beta,\mu}$ can be written in terms of the Christoffel symbols (2.12):

$$g_{\alpha\beta,\mu}\frac{p^\alpha p^\beta p^\mu}{2p_0}=\Gamma_{\alpha\beta\mu}\frac{p^\alpha p^\beta p^\mu}{p_0}, \tag{A6}$$

while the two terms inside the square bracket on the first line of Eq. (A5) can be related to the covariant derivative of $\omega_\nu^{\hat{\jmath}}$:

$$\begin{aligned}&-p^\mu p^\nu\frac{\partial\omega_\nu^{\hat{\imath}}}{\partial x^\mu}+\Gamma^{j}{}_{\mu\nu}p^\mu p^\nu\omega_j^{\hat{\imath}}\\&\quad=-p^\mu p^\nu\nabla_\mu\omega_\nu^{\hat{\imath}}-\Gamma^0{}_{\mu\nu}p^\mu p^\nu\omega_0^{\hat{\imath}},\end{aligned} \tag{A7}$$

which can be written in terms of the connection coefficients (2.14):

$$\nabla_\mu\omega_\nu^{\hat{\jmath}}=\omega_\mu^{\hat{\beta}}\nabla_{\hat{\beta}}\omega_\nu^{\hat{\jmath}}=-\Gamma^{\hat{\jmath}}{}_{\hat{\alpha}\hat{\beta}}\omega_\nu^{\hat{\alpha}}\omega_\mu^{\hat{\beta}}. \tag{A8}$$

Inserting Eqs. (A6), (A7) and (A8) into Eq. (A5) gives the final form for the Boltzmann equation:

$$p^{\hat{\alpha}}e_{\hat{\alpha}}^\mu\left(\frac{\partial f}{\partial x^\mu}\right)_{p^{\hat{\imath}}}-\Gamma^{\hat{\imath}}{}_{\hat{\alpha}\hat{\beta}}p^{\hat{\alpha}}p^{\hat{\beta}}\frac{\partial f}{\partial p^{\hat{\imath}}}=C[f]. \tag{A9}$$

APPENDIX B: CONSERVATIVE FORM OF THE BOLTZMANN EQUATION WRITTEN WITH RESPECT TO NONHOLONOMIC TETRAD FIELDS

In this section of the appendix, we present a derivation of the conservative form (2.16) of the Boltzmann equation (2.13), written with respect to nonholonomic tetrad fields. Even though the relation between these equations was already found in Ref. [23], we present this calculation here for completeness.

The term involving the spatial derivatives of f in Eq. (2.13) can be put in conservative form as follows:

$$p^{\hat{\alpha}}e_{\hat{\alpha}}^\mu\frac{\partial f}{\partial x^\mu}=\frac{1}{\sqrt{-g}}\partial_\mu(\sqrt{-g}p^{\hat{\alpha}}e_{\hat{\alpha}}^\mu f)-\Gamma^{\hat{\beta}}{}_{\hat{\alpha}\hat{\beta}}p^{\hat{\alpha}}f, \tag{B1}$$

where the connection coefficient appears from taking the covariant derivative of $e_{\hat{\alpha}}^\mu$:

$$\frac{1}{\sqrt{-g}}\partial_\mu(\sqrt{-g}e_{\hat{\alpha}}^\mu)=\nabla_\mu e_{\hat{\alpha}}^\mu=\omega_\mu^{\hat{\beta}}\Gamma^{\hat{\rho}}{}_{\hat{\alpha}\hat{\beta}}e_{\hat{\rho}}^\mu=\Gamma^{\hat{\beta}}{}_{\hat{\alpha}\hat{\beta}}. \tag{B2}$$

The second term in Eq. (2.13) can be written as

$$\begin{aligned}\Gamma^{\hat{\imath}}{}_{\hat{\alpha}\hat{\beta}}p^{\hat{\alpha}}p^{\hat{\beta}}\frac{\partial f}{\partial p^{\hat{\imath}}}&=p^{\hat{0}}\frac{\partial}{\partial p^{\hat{\imath}}}\left(\Gamma^{\hat{\imath}}{}_{\hat{\alpha}\hat{\beta}}\frac{p^{\hat{\alpha}}p^{\hat{\beta}}}{p^{\hat{0}}}f\right)\\&\quad-fp^{\hat{0}}\Gamma^{\hat{\imath}}{}_{\hat{\alpha}\hat{\beta}}\frac{\partial}{\partial p^{\hat{\imath}}}\left(\frac{p^{\hat{\alpha}}p^{\hat{\beta}}}{p^{\hat{0}}}\right).\end{aligned} \tag{B3}$$

The term on the second line in Eq. (B3) can be computed as follows. For the case when the derivative acts on $p^{\hat{\alpha}}$, the following expression is obtained:

$$\Gamma^{\hat{\imath}}{}_{\hat{\alpha}\hat{\beta}}\frac{\partial p^{\hat{\alpha}}}{\partial p^{\hat{\imath}}}=\Gamma^{\hat{\imath}}{}_{\hat{0}\hat{\beta}}\frac{p_{\hat{\imath}}}{p^{\hat{0}}}+\Gamma^{\hat{\jmath}}{}_{\hat{\jmath}\hat{\beta}} \tag{B4a}$$

$$=\Gamma^{\hat{\alpha}}{}_{\hat{0}\hat{\beta}}\frac{p_{\hat{\alpha}}}{p^{\hat{0}}} \tag{B4b}$$

$$=\Gamma^{\hat{0}}{}_{\hat{\alpha}\hat{\beta}}\frac{p^{\hat{\alpha}}}{p^{\hat{0}}}, \tag{B4c}$$

where the term $\Gamma^{\hat{\jmath}}{}_{\hat{\jmath}\hat{\beta}}$ in Eq. (B4a) vanishes due to the antisymmetry of the connection coefficients in the first two indices. Furthermore, the term $\Gamma^{\hat{\imath}}{}_{\hat{0}\hat{\beta}}p_{\hat{\imath}}=\Gamma^{\hat{\alpha}}{}_{\hat{0}\hat{\beta}}p_{\hat{\alpha}}$, since $\Gamma^{\hat{0}}{}_{\hat{0}\hat{\beta}}=0$. Finally, Eq. (B4c) can be established by noting that $\Gamma^{\hat{\alpha}}{}_{\hat{0}\hat{\beta}}p_{\hat{\alpha}}=\Gamma_{\hat{\alpha}\hat{0}\hat{\beta}}p^{\hat{\alpha}}=-\Gamma_{\hat{0}\hat{\alpha}\hat{\beta}}p^{\hat{\alpha}}=\Gamma^{\hat{0}}{}_{\hat{\alpha}\hat{\beta}}p^{\hat{\alpha}}$.

Next, the term involving the derivative of $p^{\hat{\beta}}$ can be expressed as

$$\Gamma^{\hat{\imath}}{}_{\hat{\alpha}\hat{\beta}}\frac{\partial p^{\hat{\beta}}}{\partial p^{\hat{\imath}}}=\Gamma^{\hat{\imath}}{}_{\hat{\alpha}\hat{0}}\frac{p_{\hat{\imath}}}{p^{\hat{0}}}+\Gamma^{\hat{\imath}}{}_{\hat{\alpha}\hat{\imath}} \tag{B5a}$$

$$=\Gamma_{\hat{\beta}\hat{\alpha}\hat{0}}\frac{p^{\hat{\beta}}}{p^{\hat{0}}}+\Gamma^{\hat{\beta}}{}_{\hat{\alpha}\hat{\beta}}, \tag{B5b}$$

where the relation $\Gamma^{\hat{\imath}}{}_{\hat{\alpha}\hat{0}}p_{\hat{\imath}}=\Gamma_{\hat{\beta}\hat{\alpha}\hat{0}}p^{\hat{\beta}}+\Gamma^{\hat{0}}{}_{\hat{\alpha}\hat{0}}p^{\hat{0}}$ was used.

Finally, the term involving the derivative of $p^{\hat{0}}$ can be computed as follows:

$$\Gamma^{\hat{\imath}}{}_{\hat{\alpha}\hat{\beta}}\frac{\partial}{\partial p^{\hat{\imath}}}\left(\frac{1}{p^{\hat{0}}}\right)=-\Gamma^{\hat{\imath}}{}_{\hat{\alpha}\hat{\beta}}\frac{p_{\hat{\imath}}}{(p^{\hat{0}})^3} \tag{B6a}$$

$$=-\Gamma_{\hat{\gamma}\hat{\alpha}\hat{\beta}}\frac{p^{\hat{\gamma}}}{(p^{\hat{0}})^3}-\Gamma^{\hat{0}}{}_{\hat{\alpha}\hat{\beta}}\frac{1}{(p^{\hat{0}})^2}. \tag{B6b}$$

Inserting Eqs. (B4c), (B5b) and (B6b) into Eq. (B3) yields:

$$\Gamma^{\hat{\imath}}{}_{\hat{\alpha}\hat{\beta}}p^{\hat{\alpha}}p^{\hat{\beta}}\frac{\partial f}{\partial p^{\hat{\imath}}}=p^{\hat{0}}\frac{\partial}{\partial p^{\hat{\imath}}}\left(\Gamma^{\hat{\imath}}{}_{\hat{\alpha}\hat{\beta}}\frac{p^{\hat{\alpha}}p^{\hat{\beta}}}{p^{\hat{0}}}f\right)+\Gamma^{\hat{\beta}}{}_{\hat{\alpha}\hat{\beta}}p^{\hat{\alpha}}f. \tag{B7}$$

The final result is obtained by substituting Eqs. (B1) and (B7) into Eq. (A9):

$$\frac{1}{\sqrt{-g}}\partial_\mu(\sqrt{-g}p^{\hat{\alpha}}e_{\hat{\alpha}}^\mu f)-p^{\hat{0}}\frac{\partial}{\partial p^{\hat{\imath}}}\left(\Gamma^{\hat{\imath}}{}_{\hat{\alpha}\hat{\beta}}\frac{p^{\hat{\alpha}}p^{\hat{\beta}}}{p^{\hat{0}}}f\right)=C[f]. \tag{B8}$$

APPENDIX C: TRANSPORT COEFFICIENTS IN THE MARLE MODEL OBTAINED VIA DE CHAPMAN-ENSKOG EXPANSION

The simplified version of the Chapman-Enskog procedure is performed in three steps, which are described below.

1. First step

In the first step, f is considered to be close to $f^{(\mathrm{eq})}$, in which case it can be written as

$$f = f^{(\mathrm{eq})}(1+\phi), \tag{C1}$$

where ϕ is regarded as a small number. Similarly, the relaxation time τ is also considered to be small, such that the leading contribution on the left-hand side of Eq. (2.29) is given by $f^{(\mathrm{eq})}$:

$$\nabla_\mu p^{\hat{\alpha}} e^\mu_{\hat{\alpha}} f^{(\mathrm{eq})} - p^{\hat{0}} \frac{\partial}{\partial p^{\hat{i}}}\left(\Gamma^{\hat{i}}{}_{\hat{\alpha}\hat{\beta}} \frac{p^{\hat{\alpha}} p^{\hat{\beta}}}{p^{\hat{0}}} f^{(\mathrm{eq})}\right) = -\frac{m}{\tau} f^{(\mathrm{eq})}\phi. \tag{C2}$$

Starting from Eq. (2.22), $f^{(\mathrm{eq})}$ can be written in terms of the "equilibrium" particle number density n_E, macroscopic velocity $u^{\hat{\alpha}}_E$ and inverse temperature β_E as follows [6]:

$$f^{(\mathrm{eq})} = \frac{n_E \beta_E}{4\pi m^2 K_2(m\beta_E)} \exp\left(\beta_E p_{\hat{\alpha}} u^{\hat{\alpha}}_E\right). \tag{C3}$$

According to Eqs. (2.31), $n_E = n$ and $u^{\hat{\alpha}}_E = u^{\hat{\alpha}}$, where n and $u^{\hat{\alpha}}$ are defined by $N^{\hat{\alpha}}$ (2.24a), which is obtained by integrating f. In order to obtain the definition of β_E, it is instructive to consider the expression of the equilibrium SET, which can be obtained by substituting $f^{(\mathrm{eq})}$ given by Eq. (C3) into Eq. (2.18), with $n = 1$:

$$T^{\hat{\alpha}\hat{\beta}}_E = E_E u^{\hat{\alpha}} u^{\hat{\beta}} + P_E \Delta^{\hat{\alpha}\hat{\beta}}, \tag{C4}$$

where $\Delta^{\hat{\alpha}\hat{\beta}} = \eta^{\hat{\alpha}\hat{\beta}} + u^{\hat{\alpha}} u^{\hat{\beta}}$ is the projector corresponding to the hypersurface orthogonal to $u^{\hat{\alpha}}$, while the equilibrium energy density E_E and pressure P_E are given by

$$E_E = nmG(\zeta_E) - P_E, \tag{C5a}$$

$$P_E = \frac{n}{\beta_E}. \tag{C5b}$$

In the above, $\zeta_E = m\beta_E$ is the relativistic coldness [6,27], while $G(\zeta_E)$ is defined in terms of modified Bessel functions of the third kind K_n [6]:

$$G(\zeta_E) = \frac{K_3(\zeta_E)}{K_2(\zeta_E)}. \tag{C6}$$

Thus, the inverse temperature β_E uniquely determines the energy density E_E and hydrostatic pressure P through Eqs. (C5). Furthermore, substituting Eqs. (C5) into Eq. (2.32) allows β_E to be written in terms of quantities derived from f:

$$nm\frac{K_1(\zeta_E)}{K_2(\zeta_E)} = E - 3(P + \overline{\omega}). \tag{C7}$$

2. Second step

In the second step, Eq. (2.20) is used to determine the evolution equations of the equilibrium quantities n, $u^{\hat{\alpha}}$ and E_E:

$$Dn = -n\nabla_{\hat{\gamma}} u^{\hat{\gamma}}, \tag{C8a}$$

$$Du^{\hat{\alpha}} = -\frac{1}{E_E + P_E}\Delta^{\hat{\alpha}\hat{\gamma}}\nabla_{\hat{\gamma}} P_E, \tag{C8b}$$

$$DE_E = -(E_E + P_E)\nabla_{\hat{\gamma}} u^{\hat{\gamma}}, \tag{C8c}$$

where

$$D \equiv u^{\hat{\gamma}}\nabla_{\hat{\gamma}} \tag{C9}$$

is the convective derivative [6,27]. Combining Eqs. (C8a) and (C8c), the convective derivative of the equilibrium temperature $T_E = \beta_E^{-1}$ can be obtained:

$$DT_E = -\frac{1}{\beta_E c_{v;E}}\nabla_{\hat{\gamma}} u^{\hat{\gamma}}, \tag{C10}$$

where $c_{v;E} \equiv \frac{1}{n}(\partial E_E/\partial T_E)$ is the heat capacity, which has the following expression:

$$c_{v,E} = \zeta_E^2 + 5\zeta_E G_E - \zeta_E^2 G_E^2 - 1, \tag{C11}$$

where $G_E \equiv G(\zeta_E)$ is defined in Eq. (C6).

3. Third step

In the third step, the nonequilibrium part $\delta T^{\hat{\alpha}\hat{\beta}} \equiv T^{\hat{\alpha}\hat{\beta}} - T^{\hat{\alpha}\hat{\beta}}_E$ of the SET is calculated by integrating Eq. (C2) after a multiplication by $p^{\hat{\alpha}} p^{\hat{\beta}}$:

$$-\frac{m}{\tau}\delta T^{\hat{\alpha}\hat{\beta}} = \nabla_{\hat{\gamma}} T^{\hat{\alpha}\hat{\beta}\hat{\gamma}}_E. \tag{C12}$$

The third order moment $T^{\hat{\alpha}\hat{\beta}\hat{\gamma}}_E$ of $f^{(\mathrm{eq})}$ is known analytically and has the following expression [6]:

$$T_E^{\hat{\alpha}\hat{\beta}\hat{\gamma}} = nm^2\left[\frac{K_4(\zeta_E)}{K_2(\zeta_E)}u^{\hat{\alpha}}u^{\hat{\beta}}u^{\hat{\gamma}} + \frac{G_E}{\zeta_E}(u^{\hat{\alpha}}\eta^{\hat{\beta}\hat{\gamma}} + u^{\hat{\beta}}\eta^{\hat{\gamma}\hat{\alpha}} + u^{\hat{\gamma}}\eta^{\hat{\alpha}\hat{\beta}})\right]. \quad \text{(C13)}$$

Performing the contractions in Eqs. (2.25) on Eq. (C12) gives

$$-\frac{1}{\tau}(E - E_E) = nD\left(\frac{3G_E}{\beta_E}\right) - 2P_E G_E\frac{Dn}{n}, \quad \text{(C14a)}$$

$$-\frac{1}{\tau}(P + \overline{\omega} - P_E) = nD\left(\frac{G_E}{\beta_E}\right) + \frac{2}{3}P_E G_E\nabla_{\hat{\gamma}}u^{\hat{\gamma}}, \quad \text{(C14b)}$$

$$-\frac{1}{\tau}q^{\hat{\gamma}} = nm\left(1 + \frac{5G_E}{m\beta_E}\right)Du^{\hat{\gamma}} + \Delta^{\hat{\gamma}\hat{\beta}}\nabla_{\hat{\beta}}\left(\frac{E_E + P_E}{m\beta_E}\right), \quad \text{(C14c)}$$

$$-\frac{1}{\tau}\pi^{\hat{\alpha}\hat{\beta}} = 2P_E G_E\nabla^{\langle\hat{\alpha}}u^{\hat{\beta}\rangle}. \quad \text{(C14d)}$$

Replacing the convective derivative Dn from Eq. (C14a) with the right-hand side of Eq. (C8a) shows that Eq. (2.32) indeed holds, allowing $\overline{\omega}$ to be cast in the form:

$$\overline{\omega} = \frac{1}{3}(E - E_E) - (P - P_E). \quad \text{(C15)}$$

The difference $P - P_E$ can be expressed in terms of the difference $E - E_E$ by expanding E in powers of $\beta^{-1} - \beta_E^{-1}$, and retaining only the first order term, as follows [6]:

$$E - E_E = (P - P_E)c_{v,E} + \cdots. \quad \text{(C16)}$$

Substituting Eq. (C16) in Eq. (C15) gives (to first order in $\beta^{-1} - \beta_E^{-1}$)

$$\overline{\omega} = \frac{c_{v,E} - 3}{3c_{v,E}}(E - E_E). \quad \text{(C17)}$$

A tedious but straightforward calculation, involving the use of Eqs. (C8a) and (C10) to eliminate the convective derivatives in Eq. (C14a), yields the following expression for the coefficient of bulk viscosity:

$$\eta = \frac{\tau P_E(3 - c_{v,E})}{3c_{v,E}^2}(20G_E + 3\zeta_E - 3\zeta_E G_E^2 - 2\zeta_E^2 G_E - 10\zeta_E G_E^2 + 2\zeta_E^2 G_E^3). \quad \text{(C18)}$$

To set Eq. (C14c) in the form in Eq. (2.27b), the convective derivative $Du^{\hat{\gamma}}$ can be replaced using Eq. (C8b), while the following identities can be employed in the second term:

$$\Delta^{\hat{\gamma}\hat{\beta}}\nabla_{\hat{\beta}}\left(\frac{E_E + P_E}{m\beta_E}\right) = \Delta^{\hat{\gamma}\hat{\beta}}\nabla_{\hat{\beta}}(P_E G_E) = \Delta^{\hat{\gamma}\hat{\beta}}\left[G_E\nabla_{\hat{\beta}}P_E + \frac{1}{m}(c_{v;E} + 1)\nabla_{\hat{\beta}}T_E\right]. \quad \text{(C19)}$$

The coefficient of thermal conductivity can now be obtained:

$$\lambda = \frac{\tau P_E}{m}(1 + c_{v;E}). \quad \text{(C20)}$$

Finally, the coefficient of shear viscosity can be read by comparing Eqs. (2.25d) and (C14d):

$$\mu = \tau P_E G_E. \quad \text{(C21)}$$

[1] M. Casals, S. R. Dolan, B. C. Nolan, A. C. Ottewill, and E. Winstanley, Phys. Rev. D **87**, 064027 (2013).
[2] A. Vilenkin, Phys. Lett. **80B**, 150 (1978).
[3] A. Vilenkin, Phys. Rev. D **21**, 2260 (1980).
[4] J. R. Letaw and J. D. Pfautsch, Phys. Rev. D **22**, 1345 (1980).
[5] B. R. Iyer, Phys. Rev. D **26**, 1900 (1982).
[6] C. Cercignani and G. M. Kremer, *The Relativistic Boltzmann Equation: Theory and Applications* (Birkhäuser Verlag, Basel, Switzerland, 2002).
[7] G. Duffy and A. C. Ottewill, Phys. Rev. D **67**, 044002 (2003).
[8] F. Becattini and F. Piccinini, Ann. Phys. (Amsterdam) **323**, 2452 (2008).
[9] F. Becattini and L. Tinti, Ann. Phys. (Amsterdam) **325**, 1566 (2010).
[10] F. Becattini, Phys. Part. Nucl. Lett. **8**, 801 (2011); *Proceedings of The International Workshop on Dense Nuclear Matter DM2010, Stellenbosh Institute for Advanced Studies (STIAS), Cape Town, South Africa, 2010*, https://wwwinfo.jinr.ru/publish/Pepan_letters/panl_2011_8/01_bec.pdf.
[11] F. Becattini and L. Tinti, Phys. Rev. D **84**, 025013 (2011).
[12] F. Becattini and L. Tinti, Phys. Rev. D **87**, 025029 (2013).

[13] F. Becattini and L. Tinti, Int. J. Geom. Methods Mod. Phys. **11**, 1450020 (2014).
[14] V. E. Ambruş and E. Winstanley, Phys. Lett. B **734**, 296 (2014).
[15] F. Becattini and E. Grossi, Phys. Rev. D **92**, 045037 (2015).
[16] D. Alba, H. W. Crater, and L. Lusanna, Int. J. Geom. Methods Mod. Phys. **12**, 1550049 (2015).
[17] V. E. Ambruş and R. Blaga, Ann. West Univ. Timisoara, Phys. **58**, 89 (2015).
[18] V. E. Ambruş and E. Winstanley, AIP Conf. Proc. **1694**, 020011 (2015).
[19] V. E. Ambruş and E. Winstanley, Phys. Rev. D **93**, 104014 (2016).
[20] C. Marle, Annales de l'I. H. P. Physique théorique **10**, 67 (1969).
[21] R. W. Lindquist, Ann. Phys. (N.Y.) **37**, 487 (1966).
[22] H. Riffert, Astrophys. J. **310** 729 (1986).
[23] C. Y. Cardall, E. Endeve, and A. Mezzacappa, Phys. Rev. D **88**, 023011 (2013).
[24] C. W. Misner, K. S. Thorne, and J. A. Wheeler, *Gravitation* (W. H. Freeman, San Francisco, 1973).
[25] G. M. Kremer, J. Stat. Mech. (2013) P04016; (2013) E05001; (2013) E10001.
[26] G. M. Kremer, Int. J. Geom. Methods Mod. Phys. **11**, 1460005 (2014).
[27] L. Rezzolla and O. Zanotti, *Relativistic Hydrodynamics* (Oxford University Press, Oxford, England, 2013).
[28] W. K. Tung, *Group Theory in Physics* (World Scientific Publishing, Philadelphia, PA, 1984).
[29] R. L. Liboff, *Kinetic Theory: Classical, Quantum and Relativistic Descriptions*, 3rd ed. (Springer-Verlag, New York, 2003).
[30] P. Romatschke, Phys. Rev. D **85**, 065012 (2012).
[31] W. Florkowski and E. Maksymiuk, J. Phys. G **42**, 045106 (2015).
[32] S. R. de Groot, W. A. van Leeuwen, and Ch. G. van Weert, *Relativistic Kinetic Theory—Principles and Applications* (North-Holland Publishing Company, Amsterdam, 1980).
[33] F. Becattini, Phys. Rev. Lett. **108**, 244502 (2012).
[34] F. Becattini, L. Bucciantini, E. Grossi, and L. Tinti, Eur. Phys. J. C **75**, 191 (2015).
[35] F. Becattini, Acta Phys. Pol. B **47**, 1819 (2016).
[36] C. Eckart, Phys. Rev. **58**, 919 (1940).
[37] W. Florkowski, *Phenomenology of Ultra-Relativistic Heavy-Ion Collisions* (World Scientific, Singapore, 2010).
[38] J. L. Anderson and H. R. Witting, Physica (Amsterdam) **74**, 489 (1974).
[39] Y. Hatta and T. Kunihiro, Ann. Phys. (Berlin) **298**, 24 (2002).
[40] T. Kunihiro and K. Tsumura, J. Phys. A **39**, 8089 (2006).
[41] T. Tsumura, T. Kunihiro, and K. Ohnishi, Phys. Lett. B **646**, 134 (2007).
[42] J. L. Anderson and H. R. Witting, Physica (Amsterdam) **74**, 466 (1974).
[43] M. Abramowitz and I. A. Stegun, *Handbook of Mathematical Functions* (National Bureau of Standards, Washington, DC, 1972).
[44] F. W. J. Olver, D. W. Lozier, R. F. Boisvert, and C. W. Clark, *NIST Handbook of Mathematical Functions* (Cambridge University Press, New York, 2010).
[45] R. C. Tolman, Phys. Rev. **35**, 904 (1930).
[46] R. C. Tolman and P. Ehrenfest, Phys. Rev. **36**, 1791 (1930).
[47] G. Pascu, arXiv:1211.2363v1.
[48] N. Nicolaevici, Classical Quantum Gravity **18**, 5407 (2001).
[49] V. E. Ambruş, arXiv:1608.01400.
[50] V. E. Ambruş and E. Winstanley, AIP Conf. Proc. **1634**, 40 (2014).
[51] R. Panerai, Phys. Rev. D **93**, 104021 (2016).